Reply to referee # 1

October 14, 2020

Dear referee,

thank you very much for your comments and suggestions on our manuscript. In the following we reply to your comments point-by-point. The indicated pages of the answers relate to the discussion paper.

1 Major concerns

As mentioned above the study is strongly linked to the work by Winterstein et al. (2019). Unfortunately, both studies have been conducted with different model versions. Moreover, the reference simulation for the MLO, REF QFLX, has been performed using a third model version / set-up. I have a hard time understanding why the authors did not simply apply the same model version as in Winterstein et al. (2019)? The authors want to make us believe that the model modifications do not have a significant impact on the outcome and try to circumvent this issue by showing differences of differences, whichby the way does not increase readability, but how can you be sure that the climate background state has no impact on the modelled response to 2x (5x) methane (CH_4)?

We would like to clarify that the slow feedbacks can only be assessed as the shown difference of differences even if exactly the same model version was used. They are defined as the SST-driven contribution to the overall response and can therefore only be assessed as the difference of the overall response (as simulated in the MLO simulations) and the rapid adjustments (as simulated in the fSST simulations). We feel that we have not stated this clearly enough in the previous manuscript. We will state this in the introduction (see remark to line 6) and at the beginning of Sect. 3.3.1 (line 179 ff, see below).
The MLO simulations were performed at a later time than the fSST simulations. The submodel MLOCEAN was not yet implemented in its full functionality in the model version used for the fSST simulations and backporting was not reasonable due to other changes in the model. Therefore, and also considering the computational cost of the simulations, we decided to run the MLO simulations with the most advanced cleanly defined model version available at that time.
Yes, we find differences in the simulated reference states of REF MLO and REF fSST (as shown for e.g. ozone (O_3) in Fig. S19), but these differences are small enough that they do not affect the conclusions about the differences between the full response and the rapid adjustments, i.e. the slow feedbacks.

Old, l. 179 ff Winterstein et al. (2019) analysed the quasi-instantaneous impact of doubled and fivefold CH_4 mixing ratios on the chemical composition of the atmosphere. In this section we investigate how tropospheric warming and associated climate feedbacks (see Sect. 3.2) modify these rapid adjustment patterns. For this purpose the difference patterns of the mixed layer ocean (MLO) sensitivity simulations are compared to those of the fSST simulations.

New, l. 179 ff Winterstein et al. (2019) analysed the quasi-instantaneous impact of doubled and fivefold CH_4 mixing ratios on the chemical composition of the atmosphere. In this section we investigate the respective slow feedbacks that are assessed as the difference between the full response (as simulated in the MLO simulations) and the rapid adjustments (as simulated in the fSST simulations) and therefore visualized as differences of the differences.

As already mentioned above the presentation of the results is strongly linked to the paper by Winterstein et al. (2019). Without knowing that paper, I find it often very difficult to follow the argumentation. For example, the paper discusses on increase in SWV due to enhanced atmospheric methane, but Fig. 6 displays negative changes in SWV as it present the difference SWV response in the MLO and fSST runs. This way of presenting the results is not very intuitive as the reader first has to look into the supplement to find the SWV response to enhanced CH_4 in the MLO runs and then has to think about differences between the fSST and the MLO set-up. For the sake of readability and clarity I suggest to re-structure the paper as follows: First present the results of the MLO runs and move several of the figures provided in the supplement to the main paper, and then discuss the differences to Winterstein et al. (2019), maybe only for one case (2x or 5x), if the paper turns out to become too long.

We understand that it is difficult to follow the presentation of the previous structure without knowing Winterstein et al. (2019). Therefore, we will make the following changes.

- We will add a short summary of the most important findings and conclusions of Winterstein et al. (2019) in the introduction (see remark to line 6). This implies that we do not need to refer to Winterstein et al. (2019) in the results section too often. We will review the results section with regard to this.
- We will show panel plots of the overall response (MLO) and slow feedbacks (difference between MLO and fSST) for temperature, hydroxyl radical (OH), water vapour (H_2O), and O_3. This should make it easier to interpret the slow response in comparison to the full response.
- We will also include a short description of the full response where we think it is necessary, e.g. for O_3. However, as the slow feedbacks represent only small modifications of the rapid adjustments, we think that it is not necessary to discuss the full response separated from the slow feedbacks and, that it would largely repeat the study of Winterstein et al. (2019).

The argumentation is often very qualitative, but not quantitative. A good example is the discussion of SWV changes and their attribution to changes in CPT and CH_4 oxidations. The CPT changes could be transferred into a change in H2O entry values, and from the model simulations it should be easy to calculate SWV production from CH_4 oxidation. With that, the importance of both effects could be quantified. This is only one example, but there are several places where some more quantification would be desirable.

We agree that more quantification would be desirable. Therefore, we went through the manuscript and have the following suggestions for improvement, first regarding the discussion about the H_2O response:

- We had already included the relative change of H_2O entry values in l. 273, but we will also include the absolute values in ppm as these might be more relevant. We have estimated the H_2O entry value as the tropical (10°S–10°N) mean H_2O mixing ratio at 70 hPa following Revell et al. (2016).
- The quantification of stratospheric water vapour (SWV) production from CH_4 oxidation is not so straightforward. It has often been assumed that two H_2O molecules result from one oxidized CH_4 molecule, but Frank et al. (2018) showed that the yield deviates from two molecules and further varies with height. Tracing the chemical pathways to determine the actual yield of H_2O is not so trivial and requires a comprehensive tagging mechanism (see also Frank et al., 2018). Another possibility is to estimate H_2O from CH_4 oxidation as $H_2O_{CH4} = H_2O - H_2O_{entry}$. We have already done this qualitatively when we compared the change of H_2O entry mixing ratio that is slightly higher in the MLO runs with the response of H_2O in the middle and upper stratosphere that is lower in the MLO runs. We will calculate it explicitly with the formula above and include a Figure in the supplement.

Old, l. 271 ff The SWV mixing ratio at a given location and time can be approximated as the sum of these two terms (Austin et al., 2007; Revell et al., 2016). We calculate the amount of tropospheric H_2O entering the stratosphere as the tropical (10°N–10°S) mean H_2O mixing ratio at 70 hPa following Revell et al. (2016). The H_2O entry mixing ratio increases by about 10 % (40 %) in the CH_4 doubling (fivefolding) experiments (both MLO and fSST). The relative increases are insignificantly higher in both MLO experiments compared to the respective fSST experiment. Furthermore, the zonal mean tropical cold point temperature (CPT) increases in all sensitivity simulations (see Fig. S9). The magnitude and the latitude dependence of the CPT changes are very similar for both doubling and both fivefolding experiments, although slightly larger for the MLO experiments in line with the changes of the H_2O entry mixing ratio. Changes of the amount of tropospheric H_2O entering the stratosphere can therefore not explain the differences in the SWV response between MLO and fSST in the middle and upper stratosphere. The increases of the H_2O entry mixing ratio and the CPT are both slightly stronger in the MLO experiments and would therefore suggest a stronger increase of SWV in the MLO experiments. On the contrary, the increases of SWV are weaker in the middle and upper stratosphere in the MLO experiments compared to fSST. The contribution of the CH_4 oxidation on SWV can explain these weaker increases of SWV in the MLO experiments. The strengthening of the CH_4 oxidation in the stratosphere is weaker in the MLO experiments resulting likewise in a weaker increase of SWV produced by CH_4 oxidation.

New, l. 271 ff The SWV mixing ratio at a given location and time can be approximated as the sum of these two terms following Austin et al. (2007); Revell et al. (2016) as

$$H_2O = H_2O_{\text{entry}} + H_2O_{\text{CH4}}.$$

We calculate the amount of tropospheric H_2O entering the stratosphere as the tropical (10°S–10°N) mean H_2O mixing ratio at 70 hPa following Revell et al. (2016). The H_2O entry mixing ratio increases by 9.08 % (0.14 ppm) in S2 fSST, 9.77 % (0.17 ppm) in S2 MLO, 38.53 % (0.57 ppm) in S5 MLO, and 38.86 % (0.68 ppm) in S5 MLO. Furthermore, the zonal mean tropical CPT increases in all sensitivity simulations (see Fig. S9). Though differences exist between the reference CPT in MLO und fSST, the magnitude and latitudinal structure of the CPT changes are very similar for both doubling and both fivefolding experiments. They are also a bit larger for the MLO experiments (again consistent for the S2 and S5 case), in line with the response of the H_2O entry mixing ratios. Changes of the amount of tropospheric H_2O entering the stratosphere can therefore not explain the weaker increase of SWV in the MLO experiments compared to fSST in the middle and upper stratosphere.

To illustrate the effect of CH_4 oxidation on the SWV response, Fig. S8 shows the response of H_2O from CH_4 oxidation estimated using Eq. 2. As discussed in the previous paragraph, the strengthening of the CH_4 oxidation in the stratosphere is weaker in the MLO experiments. This results in a weaker increase of SWV produced by CH_4 oxidation in the middle and upper stratosphere (see Fig. S8 c) d)) and can explain the difference of SWV response between MLO and fSST as shown in Fig. 6.

In addition, we will also include the following points:

- We will add the tropospheric CH_4 lifetime when only the temperature dependent reaction rate coefficient responds to the forcing (see remark to line 205–214).
- To quantify the composition changes in the tropical lower stratosphere we will give average values of CH_4 and O_3 changes in boxes in this region.

For CH_4:

Old, l. 238 ff Another aspect to note in Fig. 5 is the more than 5×CH_4 increase in the lowermost tropical stratosphere for S5 MLO. This feature indicates enhanced tropical upwelling, which leads to larger CH_4 mixing ratios in the tropical lower stratosphere. This feature is more pronounced in S5 MLO than in S5 fSST, in line with the more pronounced changes of tropical upwelling in the MLO set-up as discussed in Sect. 3.2.

New, l. 238 ff Another aspect to note in Fig. 5 is the more than 2× or 5×CH_4 increase in the lowermost tropical stratosphere. This feature indicates enhanced tropical upwelling, which leads to larger CH_4 mixing

ratios in the tropical lower stratosphere. It is more pronounced in the MLO than in the fSST experiments, in line with the more pronounced changes of tropical upwelling in the MLO set-up as discussed in Sect. 3.2. The average deviation from 2× or 5×CH_4 for a region in the tropical lower stratosphere (30°S–30°N, 70–20 hPa) is 0.16 % for S2 fSST, 0.37 % for S2 MLO, 0.23 % for S5 fSST, and 1.31 % for S5 MLO.

For O_3:

Old, l. 298 A dominant feature is the stronger decrease of O_3 in the lowermost tropical stratosphere in S5 MLO compared to S5 fSST of up to 18 percentage points (p.p.). This difference also exists between the S2 simulations, albeit weaker (4 p.p.).

New, l. 298 A dominant feature is the stronger decrease of O_3 in the lowermost tropical stratosphere in S5 MLO compared to S5 fSST of up to 18.39 p.p.. The average difference between S5 MLO and S5 fSST for a region in the tropical lower stratosphere (30°S–30°N, 100–20 hPa) is 6.33 p.p.. This difference also exists between the S2 simulations, albeit weaker (with a maximum difference of 4.68 p.p. and an average difference of 1.67 p.p.).

2 Specific comments

The title is very general, almost the same meaning as Winterstein et al. (2019).

We will change the title to *Slow Feedbacks Resulting from Strongly Enhanced Atmospheric Methane Concentrations in a Chemistry-Climate Model with Mixed Layer Ocean* to emphasize that this study focuses on the slow SST-driven feedbacks.

L6 and introduction: It would be nice to see a short definition/description of instantaneous and slow responses / feedbacks. Maybe it would be helpful to add a schematic to the paper, which shows the considered processes and clearly separates fast and slow effects.

While we think that the key parameters of the conceptual radiative forcing, radiative feedback, and climate sensitivity framework adopted here, have all been mentioned and defined in the original manuscript, we admit that the referee's proposal of a compact presentation in the introduction is certainly worthwhile. To account for the referee's request, we have reorganized and somewhat extended the introduction, starting at l.42. However, since our manuscript already contains a lot of Figures, we tend to not include an additional schematic.

Old, l. 42 However, these studies did not focus on the climate impact of CH_4. Other recent studies assessing climate feedbacks and climate sensitivity of CH_4 did not include radiative contributions from chemical feedbacks in their analysis (Modak et al., 2018; Smith et al., 2018; Richardson et al., 2019).

Winterstein et al. (2019) assessed chemical feedback processes and their radiative impact (RI) in sensitivity simulations forced by 2-fold (2×) and 5-fold (5×) present-day (year 2010) CH_4 mixing ratios. As their simulation set-up prescribed sea surface temperatures (SSTs) and sea ice concentrations (SICs) and thus suppressed surface temperature changes, the parameter changes in their simulations have the character of rapid adjustments (e.g., Forster et al., 2016; Smith et al., 2018). In the effective radiative forcing (ERF) framework, rapid adjustments of radiatively active species are counted as part of the forcing and are to be distinguished from slow climate feedbacks that are coupled to surface temperature changes (Sherwood et al., 2015). Climate sensitivity parameters, reflecting the degree of surface temperature change per unit forcing, have been found to be less dependent on the forcing agent with this definition compared to previous definitions of radiative forcing (RF) (e.g., Shine et al., 2003; Hansen et al., 2005; Richardson et al., 2019).

As a follow-up on Winterstein et al. (2019), we assess the respective SST-driven climate feedbacks, their effect on the quasi-instantaneous response of the chemical composition, and consequently resulting radiative feedbacks. Consistent with Winterstein et al. (2019), we perform sensitivity simulations with 2× and 5× present-day CH_4 mixing ratios with the ECHAM/MESSy Atmospheric Chemistry (EMAC) chemistry-climate model (CCM) (Jöckel et al., 2016), but this time coupled to a MLO model instead of prescribing SSTs and SICs. To our knowledge, this is the first study assessing the response to strong increases of CH_4 mixing ratios in a fully coupled CCM, meaning that the interactive model system includes atmospheric dynamics, atmospheric chemistry, and ocean thermodynamics.

New, l. 42 However, these studies did not focus on the climate impact of CH_4. In climate feedback and sensitivity studies it has become standard to distinguish between rapid adjustments of the system (that develop in direct reaction to the forcing, independently from sea surface temperature changes) and feedbacks driven by slowly evolving temperature changes at the Earth's surface (e.g., Colman and McAvaney, 2011; Geoffroy et al., 2014; Smith et al., 2020). Under this concept, the rapid radiative adjustments are counted as an integral part of the radiative forcing, yielding the so-called effective radiative forcing (Shine et al., 2003; Hansen et al., 2005). The concept has been found to be physically more meaningful than other radiative forcing frameworks, as the climate sensitivity parameter, i.e., the global mean surface temperature change per unit radiative forcing, is becoming less dependent on the forcing agent (Hansen et al., 2005; Sherwood et al., 2015; Richardson et al., 2019). However, recent studies of climate feedbacks and sensitivity to a CH_4 forcing adopting the effective radiative forcing concept did not account for the radiative contribution from chemical feedbacks in their analysis (Modak et al., 2018; Smith et al., 2018; Richardson et al., 2019).

Winterstein et al. (2019) assessed chemical feedback processes and their RI in simulations forced by 2-fold (2×) and 5-fold (5×) present-day (year 2010) CH_4 mixing ratios. As their simulation set-up used prescribed sea surface temperatures (SSTs) and sea ice concentrations (SICs) and thus suppressed surface temperature changes, the parameter changes in their simulations match the rapid adjustment and effective radiative forcing concept (e.g., Forster et al., 2016; Smith et al., 2018). Rapid radiative adjustments to stratospheric ozone and water vapor changes were found to make a considerable contribution to the CH_4 effective radiative forcing, in line with previous respective findings (e.g., Shindell et al., 2005, 2009; Stevenson et al., 2013). SWV mixing ratios were found to increase steadily with height under increased CH_4 in the quasi-instantaneous response as analysed by Winterstein et al. (2019). Rapid adjustments of the chemical composition of the stratosphere lead to increases of OH favoring the depletion of CH_4, which is an important in situ source of SWV. The increased SWV mixing ratios cool the stratosphere, thereby affecting O_3. In the troposphere, the enhanced CH_4 burden leads to a strong reduction of its most important sink partner, OH, thereby affecting the CH_4 lifetime. Winterstein et al. (2019) found a near-linear prolongation of the tropospheric CH_4 lifetime with increasing scaling factor of CH_4 for the two conducted experiments (2× and 5×CH_4).

As a follow-up on Winterstein et al. (2019), we assess the respective slow SST-driven response of the chemical composition and resulting radiative feedbacks. Consistent with Winterstein et al. (2019), we perform sensitivity simulations with 2× and 5× present-day CH_4 mixing ratios with the EMAC CCM (Jöckel et al., 2016), but this time coupled to a MLO model instead of prescribing SSTs and SICs. For radiative forcing strengths as discussed here, equilibrium climate sensitivity simulations using a thermodynamic mixed layer ocean as lower boundary condition have been shown to represent the surface temperature response yielded in (much more resource demanding) model setups involving a dynamic deep ocean sufficiently well (e.g., Danabasoglu and Gent, 2009; Dunne et al., 2020; Li et al., 2013). The slow feedbacks are assessed as the difference between the full response (as simulated in the MLO simulations) and the rapid adjustments (as simulated in the simulations with prescribed SSTs and SICs). To our knowledge, this is the first study assessing the response to strong increases of CH_4 mixing ratios in a fully coupled CCM, meaning that the interactive model system includes atmospheric dynamics, atmospheric chemistry, and ocean thermodynamics.

L90/91: I am bit confused by the description of the applied CH_4 boundary condition. I thought that CH_4 is relaxed towards to observational data set, and that this data set is simply multiplied by 2 (5) for the sensitivity runs. Why the "equilibrium CH_4 fields of the respective fSST simulations"? What is the

difference / advantage?

We apply the nudging of the CH_4 mixing ratio to the observational data set only at the lower boundary. The atmospheric CH_4 mixing ratios are free to adjust to this forcing. In the stratosphere, for example, the increase of CH_4 mixing ratio deviates from the increase factors of 2 and 5, respectively.
As the equilibrium fields of CH_4 mixing ratio from the fSST experiments are already close to the respective equilibrium of the MLO simulations, the initialization with these fields shortens the spin-up. We will reformulate the sentence to state this point more clearly.

Old The MLO simulations have been initialized with the equilibrium CH_4 fields of the respective fSST simulations, thus the initial CH_4 fields of S2 MLO and S5 MLO were implicitly scaled by two and five, respectively.

New The MLO simulations have been initialized with the equilibrium CH_4 fields of the respective fSST simulations. As the latter are already close to the respective equilibrium CH_4 fields of the MLO simulations, the initialization with these fields shortens the spin-up.

L91 onwards: What is the advantage / difference between the relaxation approach and simply prescribing the CH_4 concentration at the surface? What relaxation timescale is used? With the long lifetime of CH_4 there should not be a large difference?

Indeed, it is in principle the same as the relaxation time (10800 s) is short in comparison with the CH_4 lifetime and transport times. We will add the nudging coefficient to the manuscript.

Old Alike the fSST simulations, the CH_4 lower boundary mixing ratios of the MLO simulations are prescribed by Newtonian relaxation (i.e. nudging).

New Alike the fSST simulations, the CH_4 lower boundary mixing ratios of the MLO simulations are prescribed by Newtonian relaxation (i.e. nudging) with a nudging coefficient of 10800 s.

REF QFLX: This simulation should be the same as REF fSST, shouldn't it? Does REF MLO also include the gravity wave set-up as described in Appendix B? If not, do you expect any impact?

In principle, REF QFLX should be the same as REF fSST, but the simulations were performed with different model versions. ALL MLO simulations use the same gravity wave set-up as the fSST simulations for consistency. The different gravity wave set-up does mainly influence the middle atmosphere. We therefore presume that the influence on the ground is so small that the heat flux correction is not affected.

Old In the REF QFLX simulation the setting of the non-orographic gravity wave drag parameterization (GWAVE, Baumgaertner et al., 2013) was different than in the other simulations, ...

New In the REF QFLX simulation the setting of the non-orographic gravity wave drag parameterization (GWAVE, Baumgaertner et al., 2013) was different than in all the other simulations (fSST and MLO), ...

L127/128: What is the reason for the negative bias and observed total column CH_4? This is a good example where an explanation seems to be given in Winterstein et al. (2019), but is unfortunately not

summarized in the present study.

Thank you for this note. We will add a short explanation to the text.

Old, l. 127 ff Consistent with REF fSST (see Winterstein et al., 2019), there is a negative bias between the REF MLO and the observed total CH_4 columns of less than 4 % (not shown). Given that relative comparisons between sensitivity simulations and the reference are the main target of our analysis, REF MLO represents CH_4 conditions of the year 2010 sufficiently realistic for our purpose.

New, l. 127 ff Consistent with REF fSST (see Winterstein et al., 2019), there is a negative bias between the REF MLO and the observed total CH_4 columns of less than 4 % (not shown). Note that not all the observations originate precisely from the year 2010. The global annual mean CH_4 surface mixing ratios have, for example, risen by about 0.024 ppm from 2010 to 2014 (www.esrl.noaa.gov/gmd/ccgg/trends_ch4/), the year of the study by Klappenbach et al. (2015). In addition, the CH_4 lifetime could be slightly underestimated. The CH_4 lifetime in EMAC lies in the middle to lower range in comparisons with other CCMs (Jöckel et al., 2006; Voulgarakis et al., 2013). However, given that relative comparisons between sensitivity simulations and the reference are the main target of our analysis, REF MLO represents CH_4 conditions of the year 2010 sufficiently realistic.

L136/137, Fig. S1: I have also worked with the ECHAM5 MLO, and I am a bit concerned about the difference pattern shown in Fig. S1, namely the temperature difference around 60S, especially over the eastern hemisphere. In my simulation the MLO was in much better agreement with the reference SST climatology. Any thoughts about this?

We have derived the flux correction at the surface that stabilizes the MLO reference run from the surface fluxes of the fixed SST reference run. If you did likewise in your coupling exercise, one possibility could be that your basic model (with fixed SSTs) has had an ideally balanced top of the atmosphere radiation balance, with optimally low correction fluxes. (In our case the original global radiation balance was -1.14 Watt per square meter (W m^{-2}) for REF fSST.) As the largest temperature deviations occur near the ice edge, another possibility could be that you provided a multiple iteration of the correction fluxes in these regions to ensure optimal reproduction of the ice edge location in the reference run with MLO. Did you?

MLO: A more general question to the MLO: The MLO does not consider heat exchange with the deep ocean, but all forcing goes into the MLO. Up to which forcing strength is the usage of an MLO justified?

We feel that there is robust, long standing evidence for a sufficient reproduction of climate sensitivity parameters simulated by deep ocean coupled AOGCMs by MLO coupled AOGCMs in case of forcing strengths at least up to carbon dioxide (CO_2) doubling (Danabasoglu and Gent, 2009; Dunne et al., 2020). This evidence has been explicitly confirmed for the ECHAM5 climate model (Li et al., 2013), which is the atmospheric model basic to the chemistry-climate model setup used in our paper. Problems may arise for larger forcings (4xCO_2 and higher) with strong ocean mixed layer warming, which is not transferred to the deep layers, but as our forcings are much smaller than for CO_2 doubling, that should not be an issue here.
We will add a clarifying sentence to the paragraph introducing the MLO setup (l. 58, see also remark to line 6):

Old, l. 58 ... of prescribing SSTs and SICs.

New, l. 58 ... of prescribing SSTs and SICs. For radiative forcing strengths as discussed here, equilibrium climate sensitivity simulations using a thermodynamic mixed layer ocean as lower boundary condition have been shown to represent the surface temperature response yielded in (much more resource demanding) model setups involving a dynamic deep ocean sufficiently well (e.g., Danabasoglu and Gent, 2009; Dunne et al., 2020; Li et al., 2013).

L173 onwards: If Bony et al discussed a similar feature for CO_2, then why not adding a short (speculative) discussion for CH_4?

Our previous formulation was a bit vague. What we wanted to indicate is the following: Bony et al. (2013) found differences between the fast and the slow (temperature driven) response of the tropospheric tropical circulation in CO_2 increase experiments. We will state that more clearly.
However, we still think that a detailed discussion of the processes leading to these differences is beyond the scope of this paper. As proposed by the second referee, Peer Nowack, we will add an outlook on tropospheric circulation changes in CH_4 increase simulations as this is surely an interesting research question by itself.

Old, l. 173 ff A similar feature has been noticed and discussed in CO_2 increase simulations, too (e.g. Bony et al., 2013). However, ...

New, l. 173 ff Differences between the fast and the slow response of the tropospheric tropical circulation have been noticed and discussed in CO_2 increase simulations, too (e.g. Bony et al., 2013). However, ...

L205-214: It would be nice to see some more quantification of the temperature effect on the CH_4 lifetime!

Fig. 3 shows the total effect on the CH_4 lifetime that results from changes of CH_4, OH and the temperature dependent reaction rate coefficient. A possible quantification of the temperature effect on CH_4 lifetime would be the comparison with the CH_4 lifetime calculated using only a changed reaction rate coefficient corresponding to temperatures of $2\times$ and $5\times$ CH_4. However, also the abundance of OH is influenced by temperature changes as we show in this study. Therefore, changing only the reaction rate coefficient would not represent the whole temperature/climate effect on the CH_4 lifetime.
Nevertheless, we will include the isolated effect of the temperature dependent reaction rate on the CH_4 lifetime in Fig. 3.

Old, l. 205 ff Additionally, the tropospheric warming in the MLO sensitivity simulations results in a faster CH_4 oxidation as its reaction rate increases with temperature.

New, l. 205 ff Additionally, the tropospheric warming in the MLO sensitivity simulations results in a faster CH_4 oxidation as its reaction rate increases with temperature. The isolated effect of the temperature dependent reaction rate is indicated by the blue squares in Fig. 3. They show the CH_4 lifetime corresponding to REF MLO, except for the reaction rate coefficient that was calculated with temperatures corresponding to $2\times$ and $5\times$ CH_4.

L232: Why is the tropospheric CH_4 response marginally larger? Tropospheric is largely controlled by boundary condition? Remaining effect from CH_4 oxidation?

Yes, we think you are absolutely right. We will reorganize the paragraph to state this more clearly.

Old, l. 232 ff Winterstein et al. (2019) investigated whether the increase of atmospheric CH_4 follows the doubling or fivefolding for fSST conditions linearly. Tropospheric CH_4 is largely controlled by the nudging at the lower boundary through mixing and responds linearly to the increase. However, the CH_4 increase between 50 and 1 hPa has found to be smaller than a strictly linear relation would predict. This indicates enhanced chemical CH_4 depletion in the stratosphere due to changes in the chemical composition. Fig. **??** shows the relative difference between the annual zonal mean CH_4 of S2 MLO (S5 MLO) and 2× (5×) the zonal mean CH_4 of REF MLO. The doubling or fivefolding of the reference CH_4 serves to emphasize regions where the increase factor of the CH_4 mixing ratio deviates from 2 or 5, respectively. The response of tropospheric CH_4 is marginally larger than a linear increase in both MLO experiments. This is in line with the response of tropospheric CH_4 in the fSST simulations. As for the fSST simulations, the CH_4 increase in the extratropical stratosphere is weaker than a linear increase in both MLO sensitivity simulations. The non-linearity is less pronounced in the two MLO sensitivity experiments compared to the respective fSST experiments (compare with Fig. 3 in Winterstein et al., 2019) suggesting that the chemical depletion of CH_4 is enhanced in the MLO experiments as well, however, less strongly than in the fSST experiments.

New, l. 232 ff Fig. 5 shows the relative differences between the annual zonal mean CH_4 of S2 MLO (S5 MLO) and 2× (5×) the zonal mean CH_4 of REF MLO. The doubling or fivefolding of the reference CH_4 serves to emphasize regions where the increase factor of the CH_4 mixing ratio deviates from 2 or 5, respectively. The response of tropospheric CH_4 is marginally larger than a linear increase in both MLO experiments. This is in line with the response of tropospheric CH_4 in the fSST simulations. Tropospheric CH_4 is largely controlled by the nudging at the lower boundary through mixing and is, therefore, prevented to adjust to the lifetime increase as discussed above. The slightly positive values in Fig. 5 indicate a small residual of this effect. As for the fSST simulations, the CH_4 increase between 50 and 1 hPa is smaller than the factors of 2 or 5, respectively. This effect is less pronounced in the two MLO sensitivity experiments compared to the respective fSST experiments (compare with Fig. 3 in Winterstein et al., 2019) suggesting that the chemical depletion of CH_4 is enhanced in the MLO experiments as well, however, less strongly than in the fSST experiments.

L246 onwards: Again the argumentation in this section stays mainly qualitative ("weaker increases of OH are presumably connected..."). Although the arguments sound reasonable, it should be possible to keep track of chemical production / loss budgets in a CCM

Unfortunately, it is not trivial to keep track of the chemical production and loss budgets of OH in a comprehensive chemical mechanism such as MECCA. It is theoretically possible, but would require a complex tagging mechanism as presented by, e.g., Gromov et al. (2010). In the present simulations we did not use this mechanism as it is computationally expensive and can, therefore, not be applied to global simulations that cover multiple decades. For simple mechanisms, as for example the CH_4 sink reactions, keeping track of the budget is straightforward.

L293: Which one is the limiting OH precursor? Water vapor or ozone? I would imagine that depends on the atmospheric region?

As already replied to the previous remark, it is not easy to determine the production and loss budgets of OH from our simulation results. Determining the more important OH precursor is also not straightforward and would require additional calculations. Nicely et al. (2020), for example, assessed the contribution of various drivers to the CH_4 lifetime long-term trend (as proxy for OH) with a machine learning algorithm.
Here, we can only speculate if H_2O or O_3 is the limiting precursor for stratospheric OH. Our reasoning here is that, as the increase in OH is smaller in the MLO runs, while the entry of tropospheric H_2O is stronger, the limiting precursor is presumably O_3.

L297: Please add a short summary of the explanation for the O_3 response given in Winterstein et al. (2019).

We will add a short summary of the explanation for the O_3 response.

Old, l. 296 ff Winterstein et al. (2019) gave a detailed explanation of the processes leading to the resulting O_3 pattern that is also valid for the MLO simulations.

New, l. 296 ff Winterstein et al. (2019) gave a detailed explanation of the processes leading to the resulting O_3 pattern that is also valid for the MLO simulations. As the O_3 catalytic depletion cycles are less efficient at lower temperatures radiative cooling in the stratosphere results in increased O_3 mixing ratios in the middle stratosphere (between 50 and 5 hPa). Additionally, increased abundances of H_2O favor the depletion of excited oxygen ($O(^1D)$), likewise reducing the sink of O_3 and favoring increases of the O_3 abundance. Reduced O_3 mixing ratios in the lowermost tropical stratosphere indicate enhanced tropical upwelling of O_3 poor air from the troposphere into the stratosphere. Above 2 hPa, increases of OH lead to enhanced depletion of O_3 resulting in reduced O_3 mixing ratios.

Fig. S9: Would be nice to see the difference in CPT for the reference simulations, fSST and MLO, as well.

We will include the difference of cold point temperature of REF MLO and REF fSST in Fig. S9.
In addition, we will make the following change to the manuscript (see also answer to major concern 3)).

Old, l. 276 ff The magnitude and the latitude dependence of the CPT changes are very similar for both doubling and both fivefolding experiments, although slightly larger for the MLO experiments in line with the changes of the H_2O entry mixing ratio.

New, l. 276 ff Though differences exist between the reference CPT in MLO und fSST, the magnitude and latitudinal structure of the CPT changes are very similar for both doubling and both fivefolding experiments. They are also a bit larger for the MLO experiments (again consistent for the S2 and S5 case), in line with the response of the H_2O entry mixing ratios.

3 Technical corrections

Page 7, line 189, Equation (1): is there a bug in the listed units? E.g., units for reaction rate coefficient? [cm3 mol-1 s-1]? Otherwise the lifetime is not in [s].

Page 7, line 190: [kg], to be consistent with the other units.

Pages 14-15, lines 324-325: It is not necessary to additionally mention numbers listed in a table here.

Thank you for these suggestions and corrections. We fully agree and changed the manuscript accordingly. The unit of the concentration in Eq. (1) is [cm-3].

Reply to referee # 2

October 14, 2020

Dear Peer Johannes Nowack,

thank you very much for the positive comments on our manuscript. In the following we reply to your comments point-by-point. The indicated pages of the answers relate to the discussion paper.

1 Thoughts on the wider context

This work only considers the effects of increased methane in isolation, which is useful to separate its effect from those of other climate forcing agents. However, given the dependency of methane on, e.g., OH, I would expect that simultaneous CO2 forcing found in the real world could strongly interact with this picture, possibly even in a non-linear fashion. I assume that the reduction in OH driven by methane increases, for example, would be largely offset by increases in tropospheric OH under additional CO2 forcing? I am not asking that the study is revised in this sense, but the potential of such interactions should be mentioned somewhere, unless the authors can make strong arguments against this idea. A simple way to achieve this would be to add another clarifying sentence to the paragraph l. 204-214, where you discuss the importance of water vapour and ozone changes, which will also be driven by CO2 forcing and the associated tropospheric warming, thus impacting OH.

Thank you for making this point. We fully agree and will rephrase the paragraph as follows.

Old, l. 212 ... century. However, the tropospheric warming in the RCP8.5 scenario is stronger because it includes the effects of all greenhouse gass (GHGs) and not only the effect of methane (CH_4). This can explain the larger offset of the CH_4 lifetime response reported by Voulgarakis et al. (2013).

New, l. 212 ... century. However, the tropospheric warming in the RCP8.5 scenario is stronger because it includes the effects of all GHGs, as opposed to the isolated effect of CH_4 in our experiments. Additional warming induced by other GHGs, in particular carbon dioxide (CO_2), would drive water vapour (H_2O) and ozone (O_3) increases as well. Therefore, the reduction in hydroxyl radical (OH) driven by CH_4 increases in our experiments is expected to be more strongly offset under a simultaneously active CO_2 forcing.

Did the authors look at changes in the tropospheric circulation at all (cf. Chiodo Polvani 2016, Nowack et al. 2017)? I don't think any study has explored the specifics of the response to methane forcing, with its coupled effects on ozone and stratospheric water vapour before. I am NOT referring to the difference be tween the fixed SSTs and MLO runs here (Figure 2), as this might indeed beyond the scope of this work. If the model set-up allows (fairly short simulations and constrained ocean response), a short section on some central aspects of the tropospheric circulation response could further increase the impact of this paper. Otherwise, maybe suggest this point for future work with fully coupled ocean models. I could also imagine that the (lack of) tropospheric circulation changes might affect the stratospheric circulation response, e.g. through wave forcing and propagation, which might be worth commenting on

The tropospheric circulation in response to CH_4 forcing with and without interactive chemistry would be a very interesting research question, indeed. However, we think that it would open up a new subject area. Considering that this paper is already quite long, we think that a discussion about tropospheric circulation changes is beyond the scope of the present paper and we prefer to leave this point for future work. Moreover, in a future study we plan to use a CH_4 emission flux boundary condition, as opposed to the prescribed CH_4 surface mixing ratios here, so that tropospheric CH_4 can adjust to changes in its sinks. We will include a suggestion of the topic for this study in the conclusions section.

Old, l. 460 The contribution of sea surface temperature (SST)-driven climate feedbacks to the total CH_4 induced O_3 response shows remarkable similarities to the O_3 response to climate feedbacks in CO_2-forced climate change simulations (Dietmüller et al., 2014; Nowack et al., 2018; Chiodo and Polvani, 2019). The consistency between the O_3 feedbacks resulting from these different forcing agents encourages the separation of the O_3 response patterns into rapid adjustments and climate feedbacks in future studies. Rapid adjustments are specific to the forcing, whereas climate feedbacks are driven by surface temperature changes and are therefore expected to be less dependent on the forcing agent (Sherwood et al., 2015).

New, l. 460 The contribution of SST-driven climate feedbacks to the total CH_4 induced O_3 response shows remarkable similarities to the O_3 response to climate feedbacks in CO_2-forced climate change simulations (Dietmüller et al., 2014; Nowack et al., 2018; Chiodo and Polvani, 2019). The consistency between the O_3 feedbacks resulting from these different forcing agents encourages the separation of the O_3 response patterns into rapid adjustments and climate feedbacks in future studies. Rapid adjustments are specific to the forcing, whereas climate feedbacks are driven by surface temperature changes and are therefore expected to be less dependent on the forcing agent (Sherwood et al., 2015). However, the overall response of O_3 (rapid adjustments and slow feedbacks) is quite different under CH_4 forcing compared to CO_2 forcing owing to chemically induced feedbacks under CH_4 forcing. Chiodo and Polvani (2017); Nowack et al. (2017) suggested that feedbacks from interactive O_3 under CO_2 forcing have the potential to significantly alter the tropospheric circulation. As the overall O_3 response is different under CH_4 forcing, also modified feedbacks on the tropospheric circulation are expected. Those are planned to be assessed using a simulation set-up with a CH_4 emission flux boundary condition to simulate feedbacks of tropospheric CH_4 to changes in its chemical sinks.

2 Minor comments

l. 6-8: it might be the passive use of verbs that makes this paragraph slightly hard to read, or also the reference to the Winterstein et al. (2019) study. After all, all you seem to say is that: "Strong increases in CH4 reduce hydroxyl radical concentrations in the troposphere, thereby extending CH4 lifetime. We find that slow climate feedbacks counteract/dampen this effect (through increases in tropospheric water vapour and ozone(?); maybe mention the mechanism).

Thank you for this suggestion. We will modify the text as follows.

Old, l. 6 We find that the slow climate feedbacks counteract the reduction of the hydroxyl radical in the troposphere, which is caused by the strongly enhanced CH_4 mixing ratios. Thereby also the resulting prolongation of the tropospheric CH_4 lifetime is weakened compared to the quasi-instantaneous response considered previously.

New, l. 6 Strong increases of CH_4 lead to a reduction of the hydroxyl radical in the troposphere, thereby extending the CH_4 lifetime. Slow climate feedbacks counteract this reduction of OH through increases in tropospheric H_2O and O_3, thereby dampening the extension of CH_4 lifetime in comparison with the quasi-instantaneous response.

l. 11-13: Maybe more explicitly say as well that the middle-upper stratospheric changes cannot be explained by changes in cold point temperature

Thank you for this hint. We will change the text as follows.

Old, l. 11 In the middle and upper stratosphere, the increase of stratospheric water vapour is reduced with respect to the quasi-instantaneous response. Weaker increases of the hydroxyl radical cause the chemical depletion of CH_4 to be less strongly enhanced and thus the in situ source of stratospheric water vapour as well.

New, l. 11 In the middle and upper stratosphere, the increase of stratospheric water vapour is reduced with respect to the quasi-instantaneous response. We find that this difference cannot be explained by the response of the cold point and the associated H_2O entry values, but by a weaker strengthening of the in situ source of H_2O through CH_4 oxidation.

l. 25: would rephrase "influenced". After all water vapour concentrations are also influenced anthropogenically, only is the effect indirect.

Yes, this is indeed not correct. We will replace it by "directly emitted by human activity".

l. 58-60: I am fairly sure that some of the NASA-GISS simulations by Drew Shindell might have had similar model set-ups but probably looked at other research questions?

Thank you for this note. You are right, the work of Shindell et al. (2005, 2009) and Stevenson et al. (2013) should be mentioned here. We generally extended the introduction and also included these citations (see also reply to referee 1).
In addition, we will include the citation of Shindell et al. (2009) and Stevenson et al. (2013) when referring to Fig. 8.17 of the IPCC report: e.g., Fig. 8.17 in IPCC, 2013 derived from Shindell et al., 2009; Stevenson et al., 2013.

l. 85: Why not attempt a sensitivity analysis of the entire transient data following Gregory et al. GRL (2004) as well? Is the signal too small for the slope to be derived robustly? Gregory et al. A new method for diagnosing radiative forcing and climate sensitivity, Geophysical Research Letters (2004)

The signal is indeed too small for the slope to be derived robustly. We have actually tried this method and included Fig. 1 exemplary for the 5xCH4 case in this reply. For the 2xCH4 case, the signal to noise ratio is even worse.
One solution to reduce the uncertainty would be to calculate an ensemble of spin-up phases as proposed by, e.g., Ponater et al. (2012). This would be, however, computationally expensive. Therefore, we used the "fixed SST" method to quantify effective radiative forcing (ERF) as recommended by Forster et al. (2016).
We will include a short sentence in line 329, where we discuss the climate sensitivity.

Old, l. 329 Under the reasonable assumption that the total radiative impacts (RIs) from the fSST experiments represent the corresponding ERFs with chemical rapid adjustments included (Winterstein et al., 2019), we calculate the climate sensitivity parameters λ as 0.61 $\pm$ 0.17 K W^{-1} m^2 and 0.72 $\pm$ 0.07 K W^{-1} m^2, respectively.

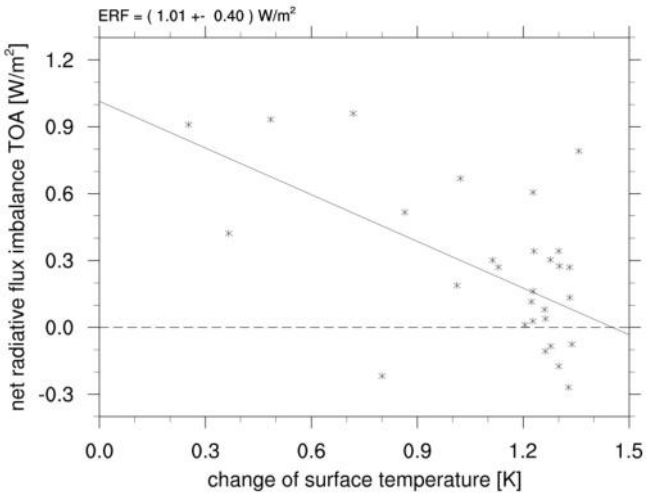

Figure 1: Regression of surface temperature response against net radiative flux perturbation at the TOA for S5 MLO following Gregory et al. (2004).

New, l. 329 The forcing strengths of 2× and 5×CH_4 turn out too small to robustly quantify the corresponding climate sensitivity parameters λ with a sensitivity analysis of the entire transient data following Gregory et al. (2004). Therefore, we calculate λ, under the reasonable assumption that the total RIs from the fSST experiments represent the corresponding ERFs with chemical rapid adjustments included (Winterstein et al., 2019), as 0.61 ± 0.17 K W^{-1} m^2 and 0.72 ± 0.07 K W^{-1} m^2, respectively.

l. 99: I suppose methane is not an emission flux then? Would be good to clarify to avoid misunderstandings.

Yes, that's right. The CH_4 mixing ratios are prescribed at the lower boundary.

We will add a clarifying sentence.

Old, l. 92 Alike the fSST simulations, the CH_4 lower boundary mixing ratios of the mixed layer ocean (MLO) simulations are prescribed by Newtonian relaxation (i.e. nudging).

New, l. 92 Alike the fSST simulations, the CH_4 lower boundary mixing ratios of the MLO simulations are prescribed by Newtonian relaxation (i.e. nudging). Thus, no CH_4 emission flux boundary was used, but pseudo surface fluxes were calculated by the MESSy submodel TNUDGE (Kerkweg et al., 2006) to reach the prescribed CH_4 lower boundary mixing ratios.

In addition, we will reformulate the following sentence.

Old, l. 99 All other prescribed boundary conditions, such as emission fluxes, in the sensitivity simulations are identical to the respective reference simulations and represent conditions of the year 2010 in general.

New, l. 99 Apart from CH_4, all other boundary conditions and emission fluxes used in the sensitivity simulations are identical to the reference simulations and represent conditions of the year 2010 in general.

l. 139: One way of quantifying the importance of the climatological surface temperature differences would be to compare the global mean surface temperatures. I assume those differences should be smaller but possibly more relevant. Given that the MLO simulations are also free-running, could those effects

also just represent some form of internal variability, which, if I understand correctly could still affect the sea ice distribution through atmospheric variability and its effect on SSTs? Higher latitudes can show similarly large variability for fully coupled ocean models. Similar arguments could apply to the NH (cf. l. 143). Looking at Fig. S1, I would think that the overall difference is positive, but the visual effect overemphasizes those changes in SH high latitudes which make up quite a small area. For climate sensitivity aspects, I would actually be more interested in the differences in tropical low-cloud regions which appear to stand out?

You are right, the differences are smaller on the global scale than at higher latitudes. The highest differences occur near the sea ice edge, which poses the largest challenge to being reproduced by a thermodynamic ocean/ice model. While avoiding to let this section become too long, we have tried to improve the balance in the discussion of regional and global differences.

Old, l. 136 The reduction of sea ice concentration (SIC) results in up to 1.5 K higher SSTs in the Southern Ocean in REF MLO compared to the prescribed climatology (see Fig. S1). Zonal mean air temperatures in the Southern Hemisphere (SH) extra-tropical troposphere are likewise up to 1 K higher in REF MLO compared to REF QFLX on annual average (not shown). As the contribution of Antarctic sea ice melting to global surface albedo feedback and climate response is comparatively small, a substantial underestimation of the climate sensitivity from this effect is not to be expected.

In the Northern Hemisphere (NH), the monthly climatology of sea ice area is generally well reproduced (see Fig. S2). However, in boreal winter and spring REF MLO overestimates the prescribed climatology of sea ice area with a maximum deviation of 1.33×10^9 km^2 in April. The larger SICs result in about 0.5 K lower SSTs on annual average in REF MLO in the Greenland Sea and in the Barents Sea (see Fig. S1), where the increase of SIC is located (not shown). In the Hudson Bay and in the Labrador Sea, on the other hand, the sea ice cover is reduced in REF MLO resulting in about 1 K higher SSTs in REF MLO compared to the prescribed climatology (see Fig. S1). The deviation from the prescribed climatology is strongest in this region in boreal summer. In summary, REF MLO simulates sufficiently realistic oceanic conditions for our purpose.

New, l. 136 The reduction of SIC results in up to 1.5 K higher SSTs in the Southern Ocean in REF MLO compared to the prescribed climatology (see Fig. S1). In the NH, the annual cycle of the sea ice area is generally well reproduced (see Fig. S2), except for a slight overestimation of the sea ice area in REF MLO resulting in about 0.5 K lower annual mean SSTs in the Greenland Sea and in the Barents Sea (see Fig. S1). However, the sign of the global and annual mean surface temperature difference between REF MLO and REF fSST is determined by the positive REF MLO bias related to the Antarctic sea ice reduction. The global mean difference is 0.28 K, much less than the regional maxima near the ice edges, and with a small contribution of about 0.10 K from the tropical belt. It is unlikely that this will lead to substantial biases in the estimation of global mean surface temperature response and climate sensitivity in the intended equilibrium climate change simulations.

l. 174/175: "would be beyond the scope"?

Yes, thank you for this suggestion. We will reformulate the sentence.

l.180: It would indeed be useful to see the overall response, the rapid adjustment response and the difference due to slow feedbacks as subplots next to each other.

We understand that our previous presentation was difficult to follow, especially when not knowing the study of Winterstein et al. (2019). We decided to show 2x2 panel plots of the full response (MLO) and the slow feedbacks (difference between MLO and fSST) for S2 and S5 for temperature, OH, H_2O, and O_3. This should simplify the interpretation of the slow response. However, we decided to not show the rapid adjustments (fSST) again as this would duplicate the work of Winterstein et al. (2019). As the slow feedbacks impose only small modifications, the patterns of the full response and the rapid adjustments are qualitatively very similar and it should be possible to follow the presentation.

l. 193: the tropopause is defined how?

Here, we used a climatological tropopause calculated as:
$\mathrm{tp_{clim}} = 300\ \mathrm{hPa} - 215\ \mathrm{hPa} \cdot \cos^2(\phi)$
The used troposphere definition is recommended by Lawrence et al. (2001), when calculating the CH_4 lifetime. We will add the following sentence to the text.

Old, l. 192 B is the region, for which the lifetime should be calculated, e.g. all grid boxes below the tropopause for the mean tropospheric lifetime.

New, l. 192 B is the region, for which the lifetime should be calculated, e.g. all grid boxes below the tropopause for the mean tropospheric lifetime. For the CH_4 lifetime calculation a climatological tropopause, defined as $\mathrm{tp_{clim}} = 300\ \mathrm{hPa} - 215\ \mathrm{hPa} \cdot \cos^2(\phi)$, with ϕ being the latitude in degree north, is used as recommended by Lawrence et al. (2001).

l. 228: revise sentence

In response to a comment by referee 1, we have restructured the whole paragraph (see answer to referee 1 to reply to line 232).

l. 258: you mean 'stratospheric abundance'

Actually, we referred to the abundance of H_2O in the troposphere and the stratosphere here. The abundance of tropospheric H_2O is indirectly influenced by CH_4 through the CH_4-induced tropospheric warming. However, we admit that the first sentence was not very meaningful and we decided to restructure the paragraph.

Old, l. 258 H_2O is a precursor of OH and its abundance is also influenced by CH_4 mixing ratios. Winterstein et al. (2019) reported a steady increase of H_2O with height for the CH_4 doubling and fivefolding experiments with prescribed SSTs and SICs. Figure 6 shows the difference of the H_2O response between the MLO and the fSST simulations (see Fig. 5 in Winterstein et al., 2019 and Fig. S8 for the respective response patterns of H_2O in the fSST and the MLO simulations, respectively). As the saturation vapour pressure increases with temperature, the warming of the troposphere in the MLO simulations consistently leads to a stronger increase of the tropospheric H_2O mixing ratio in comparison with the respective fSST simulation. The maximum difference between MLO and fSST can be found in the upper tropical troposphere and extratropical lowermost stratosphere and reaches 11 percentage points (p.p.) (35 p.p.) for the 2× (5×) CH_4 experiments.

New, l. 258 Winterstein et al. (2019) reported a steady increase of stratospheric water vapour (SWV) with height for the fSST experiments as an outcome of the enhanced CH_4 depletion as discussed in the previous

paragraph, whereas tropospheric H_2O remained largely unaffected. The warming of the troposphere in the MLO simulations consistently leads to an increase of the H_2O mixing ratios also in the troposphere as evident from Fig. 6. The maximum difference in tropospheric H_2O response between MLO and fSST can be found in the upper tropical troposphere and extratropical lowermost stratosphere and reaches 11 p.p. (35 p.p.) for the 2× (5×) CH_4 experiments.

Figure 6: another case where it would be useful to see the overall response as well instead of just the difference to the rapid adjustment response. Same for Figure 7. 2x2 panels.

Yes, we agree. As stated in the answer to the previous remark to line 180, we will show 2x2 panel plots of the full response (MLO) and the slow feedbacks (difference between MLO and fSST) for S2 and S5 for temperature, OH, H_2O, and O_3.

l. 334: the efficacy of ERF methane of close to 1 appears surprising to me – see e.g. the 145 Hansen et al. Efficacy of climate forcings, Journal of Geophysical Research (2005).

Looking at Table 1 of Hansen et al. (2005) we find efficacy values between 1.05 and 1.08 under the effective radiative forcing framework (with 1.5xCO2, equivalent to a forcing of 2.38 Wm-2 as a reference). This may seem at odds with the most recent work of Richardson et al. (2019), who suggest a CH_4 efficacy value well below 1. However, in their work the reference is 2xCO2 (equivalent to about 4 Wm-2, while the 3xCH4 simulation runs with 1.2 Wm-2 only). This is a dangerous comparison as the climate sensitivity parameter tends to depend on the strength of the forcing. Compare, e.g., with Hansen et al. (2005)'s 1.25xCO2 and 2xCO2 runs, and it becomes obvious that 3xCH4 vs. 1.25xCO2 would probably make a more fair comparison. Many recent studies also show, how delicate the climate sensitivity parameter of CO_2 can depend on the forcing strength.
We think, however, that the main difference between previous work and our study is the inclusion of ozone and water vapor contributions to the methane forcing. Thus, in a chemistry-climate model, the "effective climate sensitivity of methane" will probably contain components from pure CH_4, pure O_3, and pure stratospheric H_2O. Hence, the finding of an efficacy close to 1 in our framework is indeed a surprise that deserves further investigation.

l. 368: how is this calculation of the effect on stratospheric temperatures done precisely? Could you provide more detail about the calculations? Are they expected to be robust in different regimes of the atmosphere, e.g. in the lowermost stratosphere vs the tropical upper stratosphere? What is "addst" in equation (2)?

We feel that from our previous formulation it was not clear that the stratospheric adjusted temperature response is the one shown in Fig. 9 and Fig. S11. We will formulate this clearer and use the abbreviation ΔT_{adj} already, when introducing the calculation of stratospheric adjusted temperatures. "addst" is the EMAC internal abbreviation for the adjusted stratospheric temperatures. We agree that the naming is not very intuitive and will replace it by "adj".
The calculation of the adjusted temperatures response is regime-independent. However, it is not meaningful if the radiatively induced temperature adjustment initiates dynamic processes whose effects on the temperature field are stronger than the radiatively induced changes. This would be the case in the troposphere. However, as the stratosphere is highly stable the radiatively induced temperature response dominates. This is the case in the lower as well as in the upper stratosphere.

Old, l. 354 Following Winterstein et al. (2019) we calculate the stratospheric adjusted temperature response to changes in CH_4, tropospheric and stratospheric H_2O, and tropospheric and stratospheric O_3, as well as

their individual contributions for S2 MLO and S5 MLO (see Fig. S11 for simulation S2 MLO and Fig. 9 for simulation S5 MLO).
The difference of the adjusted stratospheric temperature response between S5 MLO and S5 fSST is shown in Fig. 10 (for S2 see Fig. S12).

New, l. 354 Following Winterstein et al. (2019) we calculate the stratospheric adjusted temperature response ΔT_{adj} to changes in CH_4, tropospheric and stratospheric H_2O, and tropospheric and stratospheric O_3, as well as their individual contributions, for S2 MLO and S5 MLO (see Fig. S11 for simulation S2 MLO and Fig. 9 for simulation S5 MLO). ΔT_{adj} represents the temperature response induced by composition changes of radiatively active gases (Stuber et al., 2001).
The difference of ΔT_{adj} between S5 MLO and S5 fSST is shown in Fig. 10 (for S2 see Fig. S12).

Old, l. 368 By calculating the difference between the total temperature response in the regular simulations and the sum of the individual contributions of CH_4, H_2O and O_3 to the adjusted stratospheric temperatures, we attempt to identify the dynamical effect ($\Delta\tilde{T}_{dyn.}$) in the stratospheric temperature response as

$$\Delta\tilde{T}_{dyn.} = \Delta T(\text{SX-REF}) - \Delta T_{addst}(\text{SX*-REF*})$$

with X being either 2 or 5. A similar approach was, for example, used by Rosier and Shine (2000) and Schnadt et al. (2002) to distinguish between the radiative impact of trace gases and dynamical contributions to the total temperature response.

New, l. 368 By calculating the difference between the total temperature response in the regular simulations ΔT and the sum of the individual contributions of CH_4, H_2O and O_3 to the adjusted stratospheric temperatures (ΔT_{adj}^{total}, see Fig. 9 a) and Fig. S11 a)), we attempt to identify the dynamical effect ($\Delta\tilde{T}_{dyn.}$) in the stratospheric temperature response as

$$\Delta\tilde{T}_{dyn.} = \Delta T(\text{SX-REF}) - \Delta T_{adj}^{total}(\text{SX*-REF*})$$

with X being either 2 or 5. A similar approach was, for example, used by Rosier and Shine (2000) and Schnadt et al. (2002) to distinguish between the radiative impact of trace gases and dynamical contributions to the total temperature response.

~~Effects of~~ Slow Feedbacks Resulting from Strongly Enhanced Atmospheric Methane Concentrations in a ~~Fully Coupled~~ Chemistry-Climate Model with Mixed Layer Ocean

Laura Stecher[1], Franziska Winterstein[1], Martin Dameris[1], Patrick Jöckel[1], Michael Ponater[1], and Markus Kunze[2]

[1]Deutsches Zentrum für Luft- und Raumfahrt (DLR), Institut für Physik der Atmosphäre, Oberpfaffenhofen, Germany
[2]Freie Universität Berlin, Berlin, Germany

Correspondence: Laura Stecher (Laura.Stecher@dlr.de)

Abstract. In a previous study the quasi-instantaneous chemical impacts (rapid adjustments) of strongly enhanced methane (CH_4) mixing ratios have been analyzed. However, to quantify the influence of the respective slow climate feedbacks on the chemical composition it is necessary to include the radiation driven temperature feedback. Therefore, we perform sensitivity simulations with doubled and fivefold present-day (year 2010) CH_4 mixing ratios with the chemistry-climate model EMAC and include in a novel set-up a mixed layer ocean model to account for tropospheric warming.

~~We find that the slow climate feedbacks counteract the~~ Strong increases of CH_4 lead to a reduction of the hydroxyl radical in the troposphere, ~~which is caused by the strongly enhanced~~ thereby extending the CH_4 ~~mixing ratios. Thereby also the resulting prolongation of the tropospheric~~ lifetime. Slow climate feedbacks counteract this reduction of the hydroxyl radical through increases in tropospheric water vapour and ozone, thereby dampening the extension of CH_4 lifetime ~~is weakened compared to~~ in comparison with the quasi-instantaneous response~~considered previously~~.

Changes in the stratospheric circulation evolve clearly with the warming of the troposphere. The Brewer-Dobson circulation strengthens, affecting the response of trace gases, such as ozone, water vapour and CH_4 in the stratosphere, and also causing stratospheric temperature changes. In the middle and upper stratosphere, the increase of stratospheric water vapour is reduced with respect to the quasi-instantaneous response. ~~Weaker increases of the hydroxyl radical cause the chemical depletion of to be less strongly enhanced and thus~~ We find that this difference cannot be explained by the response of the cold point and the associated water vapour entry values, but by a weaker strengthening of the in situ source of ~~stratospheric water vapour as well~~water vapour through CH_4 oxidation. However, in the lower stratosphere water vapour increases more strongly when tropospheric warming is accounted for enlarging its overall radiative impact. The response of the stratospheric adjusted temperatures driven by slow climate feedbacks is dominated by these increases of stratospheric water vapour, as well as strongly decreased ozone mixing ratios above the tropical tropopause, which result from enhanced tropical upwelling.

While rapid radiative adjustments from ozone and stratospheric water vapour make an essential contribution to the effective CH_4 radiative forcing, the radiative impact of the respective slow feedbacks is rather moderate. In line with this, the climate sensitivity from CH_4 changes in this chemistry-climate model setup is not significantly different from the climate sensitivity in

carbon dioxide-driven simulations, provided that the CH_4 effective radiative forcing includes the rapid adjustments from ozone and stratospheric water vapour changes.

Copyright statement. TEXT

1 Introduction

Methane (CH_4) is the second most important ~~anthropogenically influenced~~ greenhouse gas (GHG) directly emitted by human activity. Apart from its direct radiative impact (RI), CH_4 is chemically active and induces chemical feedbacks relevant for climate and air quality. Through its most important tropospheric sink, the oxidation with the hydroxyl radical (OH), it affects the oxidation capacity of the atmosphere and thus its own lifetime (e.g., Saunois et al., 2016b; Voulgarakis et al., 2013; Winterstein et al., 2019). CH_4 oxidation is further an important source of stratospheric water vapour (SWV) (e.g., Frank et al., 2018) and affects the ozone (O_3) concentration in troposphere and stratosphere via secondary feedbacks. Chemical feedbacks from O_3 and SWV contribute significantly to the total RI induced by CH_4 (e.g., Fig. 8.17 in IPCC, 2013 derived from Shindell et al., 2009 and Stevenson et al., 2013 ; Winterstein et al., 2019). The abundance of CH_4 in the atmosphere is rising rapidly at present (e.g., Nisbet et al., 2019). Furthermore, emissions from natural CH_4 sources can be prone to climate change and have the potential to strongly enhance atmospheric CH_4 concentrations (Dean et al., 2018). Together with its relevance as a GHG, the latter underlines the importance of examining implications of strongly increased CH_4 abundances in the atmosphere.

Chemistry-climate models (CCMs) are useful tools for such studies. A CCM is a General Circulation model (GCM) that is interactively coupled to a comprehensive chemistry module. This online two-way coupling is necessary to assess, on the one hand, chemically induced changes of radiatively active gases and their feedback on temperature, and on the other hand feedbacks on chemical processes driven by changes of the climatic state (e.g. temperature, circulation or precipitation). A range of CCM studies analysed the sensitivity of other atmospheric constituents, such as O_3 (Kirner et al., 2015; Morgenstern et al., 2018), SWV (Revell et al., 2016) and OH and CH_4 lifetime (Voulgarakis et al., 2013), to different projections of CH_4 mixing ratios. However, these studies did not focus on the climate impact of CH_4. ~~Other recent studies assessing~~

In climate feedback and sensitivity studies it has become standard to distinguish between rapid adjustments of the system (that develop in direct reaction to the forcing, independently from sea surface temperature changes) and feedbacks driven by slowly evolving temperature changes at the Earth's surface (e.g., Colman and McAvaney, 2011; Geoffroy et al., 2014; Smith et al., 2020) . Under this concept, the rapid radiative adjustments are counted as an integral part of the radiative forcing, yielding the so-called effective radiative forcing (ERF) (Shine et al., 2003; Hansen et al., 2005) . The concept has been found to be physically more meaningful than other radiative forcing frameworks, as the climate sensitivity parameter, i.e., the global mean surface temperature change per unit radiative forcing, is becoming less dependent on the forcing agent (Hansen et al., 2005; Sherwood et al., 2015; Richardson e However, recent studies of climate feedbacks and ~~climate sensitivity of~~ sensitivity to a CH_4 ~~did not include radiative contributions~~

forcing adopting the ERF concept did not account for the radiative contribution from chemical feedbacks in their analysis (Modak et al., 2018; Smith et al., 2018; Richardson et al., 2019).

Winterstein et al. (2019) assessed chemical feedback processes and their ~~in sensitivity~~ RI in simulations forced by 2-fold (2×) and 5-fold (5×) present-day (year 2010) CH_4 mixing ratios. As their simulation set-up ~~prescribed and~~ used prescribed sea surface temperatures (SSTs) and sea ice concentrations (SICs) and thus suppressed surface temperature changes, the parameter changes in their simulations ~~have the character of rapid adjustments (e.g., Forster et al., 2016; Smith et al., 2018) . In the~~ match the rapid adjustment and ERF ~~framework, rapid adjustments of radiatively active species are counted as part of the forcing and are to be distinguished from slow climate feedbacks that are coupled to surface temperature changes (Sherwood et al., 2015) . Climate sensitivity parameters, reflecting the degree of surface temperature change per unit forcing, have been found to be less dependent on the forcing agent with this definition compared to previous definitions of (e.g., Shine et al., 2003; Hansen et al., 2005; Richard~~ (e.g., Forster et al., 2016; Smith et al., 2018) . Rapid radiative adjustments to stratospheric O_3 and water vapour (H_2O) changes were found to make a considerable contribution to the CH_4 ERF, in line with previous respective findings (e.g., Shindell et al., 2005, 2009; SWV mixing ratios were found to increase steadily with height under increased CH_4 in the quasi-instantaneous response as analysed by Winterstein et al. (2019) . Rapid adjustments of the chemical composition of the stratosphere lead to increases of OH favoring the depletion of CH_4, which is an important in situ source of SWV. The increased SWV mixing ratios cool the stratosphere, thereby affecting O_3. In the troposphere, the enhanced CH_4 burden leads to a strong reduction of its most important sink partner, OH, thereby affecting the CH_4 lifetime. Winterstein et al. (2019) found a near-linear prolongation of the tropospheric CH_4 lifetime with increasing scaling factor of CH_4 for the two conducted experiments (2× and 5×CH_4).

As a follow-up on Winterstein et al. (2019), we assess the respective slow sea surface temperature (SST)-driven ~~climate feedbacks, their effect on the quasi-instantaneous~~ response of the chemical composition ~~, and consequently~~ and resulting radiative feedbacks. Consistent with Winterstein et al. (2019), we perform sensitivity simulations with 2× and 5× present-day CH_4 mixing ratios with the ECHAM/MESSy Atmospheric Chemistry (EMAC) CCM (Jöckel et al., 2016), but this time coupled to a mixed layer ocean (MLO) model instead of prescribing SSTs and sea ice concentrations (SICs). For radiative forcing strengths as discussed here, equilibrium climate sensitivity simulations using a thermodynamic MLO as lower boundary condition have been shown to represent the surface temperature response yielded in (much more resource demanding) model setups involving a dynamic deep ocean sufficiently well (e.g., Danabasoglu and Gent, 2009; Dunne et al., 2020; Li et al., 2013) . The slow feedbacks are assessed as the difference between the full response (as simulated in the MLO simulations) and the rapid adjustments (as simulated in the simulations with prescribed SSTs and SICs). To our knowledge, this is the first study assessing the response to strong increases of CH_4 mixing ratios in a fully coupled CCM, meaning that the interactive model system includes atmospheric dynamics, atmospheric chemistry, and ocean thermodynamics.

Our simulation strategy is explained in Sect. 2. The discussion of results in Sect. 3 starts with a brief evaluation of the reference CH_4 mixing ratio against observations and an assessment of the MLO model (Sect. 3.1), followed by the analyses of tropospheric warming and associated climate feedbacks in the MLO simulations (Sect. 3.2). In Sect. 3.3 we assess implications of SST-driven climate feedbacks on the chemical composition of the atmosphere in comparison to the quasi-instantaneous response and quantify the resulting radiative feedbacks and the climate sensitivity. We further discuss contributions from

feedbacks of radiatively active gases and from circulation changes to the stratospheric temperature response. In Sect. 4 we summarize our conclusions and give a brief outlook.

2 Description of the model and simulation strategy

We use the CCM ECHAM/MESSy Atmospheric Chemistry (EMAC; Jöckel et al., 2016) for this study. Following on from the sensitivity simulations with prescribed SSTs and SICs that were analysed by Winterstein et al. (2019), we performed a second set of sensitivity simulations with the MESSy submodel MLOCEAN (~~Kunze et al. (2014)~~ Kunze et al., 2014 ; original code by ~~Roeckner et al. (1995)~~ Roeckner et al., 1995) coupled to EMAC. The set-up of the MLO simulations is designed to follow the set-up of the simulations described by Winterstein et al. (2019) closely. We conducted all simulations at a resolution of T42L90MA, corresponding to a quadratic Gaussian grid of approximately 2.8° × 2.8° resolution in latitude and longitude and 90 levels with the uppermost level centered around 0.01 hPa in the vertical.

According to the simulation concept of Winterstein et al. (2019), we performed one reference simulation (REF MLO) and two sensitivity simulations (S2 MLO and S5 MLO) including the MLO model, all as equilibrium climate simulations. The simulations with prescribed SSTs and SICs are denoted REF fSST, S2 fSST and S5 fSST here. All simulations considered for the analysis are listed in Tab. 1. The MLO simulations have been performed with a more recent version of the Modular Earth Submodel System (MESSy; 2.54.0 instead of 2.52). The updates include changes in the chemistry module Module Efficiently Calculating the Chemistry of the Atmosphere (MECCA; ~~Sander et al. (2011)~~ Sander et al., 2011) that are discussed in Appendix A. However, inherent differences between the MLO and fSST simulations do not directly distort the evaluation, as the differences between response signals relative to the respective reference simulations, and not the direct differences between the sensitivity simulations, are analysed.

A spin-up phase of at least ten years is excluded from the analysis of each simulation to provide quasi-steady-state conditions. S2 MLO and S5 MLO were initialized from the spun-up state of REF MLO and spun-up over a 10-year period, followed by a 20-year equilibrium used for the analysis. We chose to simulate a 30-year equilibrium for the analysis of REF MLO after S2 MLO and S5 MLO branched off, so that the complete 20 years used for the analysis of S2 MLO and S5 MLO are covered by this simulation as well.

The MLO simulations have been initialized with the equilibrium CH_4 fields of the respective fSST simulations~~, thus the initial~~ . As the latter are already close to the respective equilibrium CH_4 fields of ~~S2 MLO and S5 MLO were implicitly scaled by two and five, respectively~~the MLO simulations, the initialization with these fields shortens the spin-up. Alike the fSST simulations, the CH_4 lower boundary mixing ratios of the MLO simulations are prescribed by Newtonian relaxation (i.e. nudging) ~~.~~ with a nudging coefficient of 10800 s. Thus, no CH_4 emission flux boundary was used, but pseudo surface fluxes were calculated by the MESSy submodel TNUDGE (Kerkweg et al., 2006) to reach the prescribed CH_4 lower boundary mixing ratios. The lower boundary CH_4 mixing ratios of REF MLO are nudged to the same reference as REF fSST, namely a zonal mean observation based estimate of the year 2010 from marine boundary layer sites. The observational data are provided by the Advanced Global Atmospheric Gases Experiment (AGAGE; http://agage.mit.edu/) and the National Oceanic and Atmo-

Table 1. Overview of the two sets of sensitivity simulations (fSST and MLO) with one reference simulation and two sensitivity simulations. The simulations with prescribed SSTs and SICs have already been analysed by Winterstein et al. (2019). The simulation REF QFLX is used to determine the heat flux correction for the simulations including the MLO model.

Simulation	CH_4 lower boundary	SSTs, SICs	MESSy version
REF fSST	1.8 ppmv		
S2 fSST	2 × REF fSST	prescribed (Rayner et al., 2003)	2.52
S5 fSST	5 × REF fSST		
REF MLO	1.8 ppmv	mixed layer ocean (MLO)	
S2 MLO	2 × REF MLO	MESSy submodel MLOCEAN	2.54.0
S5 MLO	5 × REF MLO		
REF QFLX	1.8 ppmv	prescribed (Rayner et al., 2003)	d2.53.0.26

spheric Administration/Earth System Research Laboratory (NOAA/ESRL; https://www.esrl.noaa.gov/). The lower boundary CH_4 mixing ratios of S2 and S5 are nudged towards the 2× and the 5× of this reference, respectively. The resulting global mean lower boundary CH_4 mixing ratio is about 1.8 parts per million volume (ppmv) for both reference simulations, 3.6 ppmv for both doubling, and 9.0 ppmv for both fivefolding experiments. ~~All other prescribed boundary conditions , such as emission fluxes ,~~ Apart from CH_4, all other boundary conditions and emission fluxes used in the sensitivity simulations are identical to the ~~respective~~ reference simulations and represent conditions of the year 2010 in general.

In the MLO simulations, the SSTs, the ice thicknesses, and the ice temperatures at ocean gridpoints are calculated by the MESSy submodel MLOCEAN. A MLO model accounts for the ocean's heat capacity without simulating the oceanic circulation explicitly. To simulate realistic SSTs with the MLO, a heat flux correction term needs to be added to the surface energy balance. We derived a monthly climatology of this heat flux correction from a control simulation with prescribed SSTs and SICs, named REF QFLX. REF QFLX uses the same monthly climatology of SSTs and SICs that was used for the fSST simulations, i. e. a monthly climatology representing the years 2000 to 2009 based on global analyses of the HadISST1 data set (Rayner et al., 2003).

In the following, the response to increased CH_4 in the MLO simulations is assessed as the difference of S2 MLO and S5 MLO with respect to REF MLO. The effects of SST-driven climate feedbacks are identified as the difference between responses in the MLO and fSST simulations. The RIs induced by changes of individual radiatively active gases are assessed using the EMAC option for multiple radiation calls in the submodel RAD (Dietmüller et al., 2016), as explained in more detail by Winterstein et al. (2019). The first radiation call receives the reference mixing ratios of all chemical species, i.e. CH_4, O_3 and H_2O. In the following radiation calls each of the species individually, and all combined, are exchanged by climatological means derived from the sensitivity simulations (S2 and S5). From these perturbed radiation fluxes the stratospheric-adjusted RI is calculated (Stuber et al., 2001; Dietmüller et al., 2016).

3 Discussion of results

3.1 Assessment of reference simulations

The simulation set-up of the reference simulation, REF MLO, aims to represent conditions typical for the year 2010. For a detailed assessment and evaluation of EMAC in general, we refer to Jöckel et al. (2016). We have evaluated the REF MLO CH_4 mixing ratios to ensure that the latter represent conditions of 2010 sufficiently realistic. The REF MLO CH_4 mixing ratios were compared to three different observational data sets that are independent from the observational estimate that serves as input for the lower boundary condition to ensure an objective evaluation. These are balloon-borne measurements conducted in the period from 1992 to 2006 from Röckmann et al. (2011), observations of a portable Fourier transform spectrometer onboard the research vessel Polarstern during a cruise from Cape Town to Bremerhaven on the Atlantic in 2014 (Klappenbach et al., 2015) and observations from the Total Carbon Column Observing Network (TCCON; Wunch et al., 2011) from the period 2009 to 2014. The vertical profile, the north-south gradient and the annual cycle of REF MLO CH_4 generally agree well with the corresponding data (not shown). Consistent with REF fSST (see Winterstein et al., 2019), there is a negative bias between the REF MLO and the observed total CH_4 columns of less than 4 % (not shown). ~~Given that~~ Note that not all the observations originate precisely from the year 2010. The global annual mean CH_4 surface mixing ratios have, for example, risen by about 0.024 ppm from 2010 to 2014 (NOAA/ESRL; https://www.esrl.noaa.gov/gmd/ccgg/trends_ch4/), the year of the study by Klappenbach et al. (2015) . In addition, the CH_4 lifetime could be slightly underestimated. The CH_4 lifetime in EMAC lies in the middle to lower range in comparisons with other CCMs (Jöckel et al., 2006; Voulgarakis et al., 2013) . However, given that relative comparisons between sensitivity simulations and the reference are the main target of our analysis, REF MLO represents CH_4 conditions of the year 2010 sufficiently realistic~~for our purpose~~.

Since this study is one of the first to use the MLOCEAN submodel in MESSy, we have carefully checked whether REF MLO reproduces SSTs and SICs of the climatology that was used to determine the heat flux correction with sufficient accuracy. The spatial pattern of the SST climatology is realistically reproduced in REF MLO (see Fig. S1). The largest differences are found at higher latitudes, where a reduction in sea ice area leads to higher SSTs, as exposed sea water is warmer than sea ice. REF MLO underestimates the monthly climatology of sea ice area in the Southern Hemisphere (SH) in all seasons, except for austral summer (see Fig. S2). The reduction of SIC results in up to 1.5 K higher SSTs in the Southern Ocean in REF MLO compared to the prescribed climatology (see Fig. S1). ~~Zonal mean air temperatures in the extra-tropical troposphere are likewise up to 1 K higher in REF MLO compared to REF QFLX on annual average (not shown). As the contribution of Antarctic sea ice melting to global surface albedo feedback and climate response is comparatively small, a substantial underestimation of the climate sensitivity from this effect is not to be expected.~~

In the Northern Hemisphere (NH), the ~~monthly climatology of~~ annual cycle of the sea ice area is generally well reproduced (see Fig. S2)~~. However, in boreal winter and spring REF MLO overestimates the prescribed climatology of~~ , except for a slight overestimation of the sea ice area ~~with a maximum deviation of 1.33×10^9 km^2 in April. The larger result in~~ in REF MLO resulting in about 0.5 K lower ~~on annual average in REF MLO in~~ annual mean SSTs in the Greenland Sea and in the Barents Sea (see Fig. ~~-~~S1)~~, where the increase of is located (not shown). In the Hudson Bay and in the Labrador Sea, on the other~~

hand, the sea ice cover is reduced in . However, the sign of the global and annual mean surface temperature difference between REF MLO resulting in about 1 K higher in and REF fSST is determined by the positive REF MLO compared to the prescribed climatology (see Fig. S1). The deviation from the prescribed climatology is strongest in this region in boreal summer. In summary, REF MLO simulates sufficiently realistic oceanic conditions for our purpose. bias related to the Antarctic sea ice reduction. The global mean difference is 0.28 K, much less than the regional maxima near the ice edges, and with a small contribution of about 0.10 K from the tropical belt. It is unlikely that this will lead to substantial biases in the estimation of global mean surface temperature response and climate sensitivity in the intended equilibrium climate change simulations.

3.2 Tropospheric temperature response and associated climate feedbacks

The tropospheric temperature response to enhanced CH_4 mixing ratios can freely develop in the MLO sensitivity simulations (see Fig. ??) 1 (a) and (b)). The temperature change patterns of S2 MLO and S5 MLO show the expected warming of the troposphere and cooling of the stratosphere (e.g., IPCC, 2013). The stratospheric cooling is less pronounced than in carbon dioxide (CO_2)-driven climate change simulations, since the CH_4 cooling is mainly caused by associated O_3 and H_2O adjustments (Kirner et al., 2015; Winterstein et al., 2019). Maximum warming in polar regions and in the upper tropical troposphere is also consistent with changes expected from increased levels of GHGs (e.g., Chap. 12 in IPCC, 2013). CH_4 doubling (fivefolding) leads to temperature increases of up to 1 K (3 K) in the Arctic on annual average. Antarctica also warms up particularly strongly in the S5 MLO scenario with a maximum warming of up to 3 K. As a result of the especially strong warming in polar regions, the sea ice area is reduced in both sensitivity simulations with respect to the reference (compare Fig. S2).

The Brewer-Dobson circulation (BDC) is expected to accelerate in a warming climate (Rind et al., 1990; Butchart and Scaife, 2001; Garcia and Randel, 2008; Butchart, 2014; Eichinger et al., 2019). Feedbacks on the chemical composition of the atmosphere, especially of the stratosphere, which result from changes of the BDC are of particular interest in this study, as they will modify the mainly chemically induced changes discussed by Winterstein et al. (2019). The BDC influences the spatial distribution of trace gases, such as O_3, H_2O, and CH_4, in the stratosphere and also their transport from the troposphere into the stratosphere (Butchart, 2014). In Fig. 2 we examine the response of the residual mean streamfunction to quantify changes of the BDC. There is indeed a strengthening of the residual mean circulation in both, S2 MLO and S5 MLO, with respect to REF MLO and it is detected in both hemispheres. The change of the residual mean streamfunction is stronger and extends to higher altitudes for the simulation S5 MLO, but the annual mean patterns are consistent in both MLO sensitivity simulations. The maximum change of about 0.7×10^9 kg s^{-1} for S5 MLO is located at about 100 hPa. Upward motion is increased in the tropics, which is balanced by an increase of downwelling between 30°–60° latitude in both hemispheres. The change of the residual mean streamfunction is stronger and reaches higher in the respective winter hemisphere in S5 MLO (see Fig. S3 and Fig. S5). The BDC response in the MLO simulations is considerably stronger than in the respective fSST sensitivity simulations. This is expected, since the main driver of changes in the BDC is tropospheric warming (Butchart, 2014). We note that changes of the residual mean streamfunction below the tropical tropopause in response to CH_4 increase exhibit different patterns in the fSST and MLO simulations (see Fig. 2). A similar feature has Differences between the fast and the slow response of the tropospheric tropical circulation have been noticed and discussed in CO_2 increase simulations,

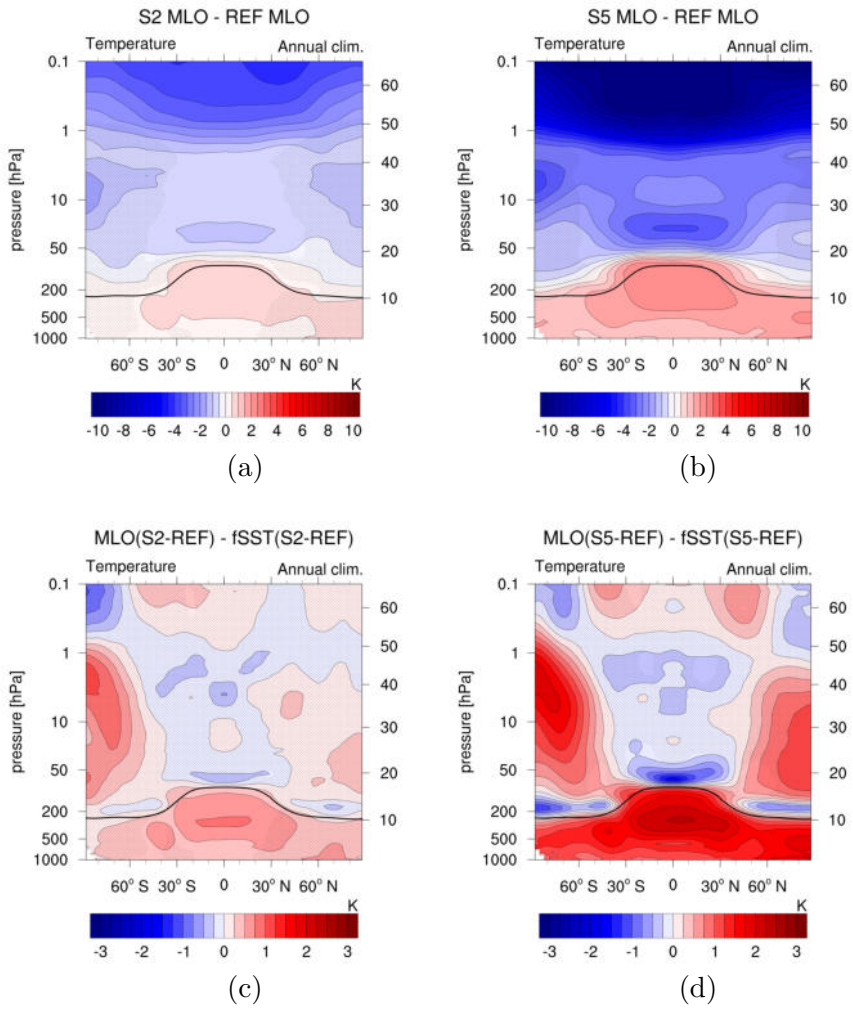

Figure 1. Upper row: Absolute annual zonal mean temperature differences between the sensitivity simulations (a) S2 MLO and (~~left~~b) ~~and~~ S5 MLO ~~(right)~~ and REF MLO in K. Lower row: Differences between the temperature response to enhanced CH_4 in the MLO and fSST set-ups in K. To calculate the latter the absolute changes of (c) S2 fSST and (d) S5 fSST are subtracted from the relative changes of S2 MLO and S5 MLO, respectively. Non-stippled areas are significant on the 95 % confidence level according to a two sided Welch's test. The solid black line indicates the climatological tropopause height of REF MLO.

too (e.g. Bony et al., 2013). However, trying to explain the origin of these tropospheric differences would ~~leave~~ be beyond the scope of the present paper, which focuses on stratospheric trace gas feedbacks to CH_4 increase. The latter are influenced by the more distinct strengthening of the BDC in the MLO experiments, as we will show in the next section.

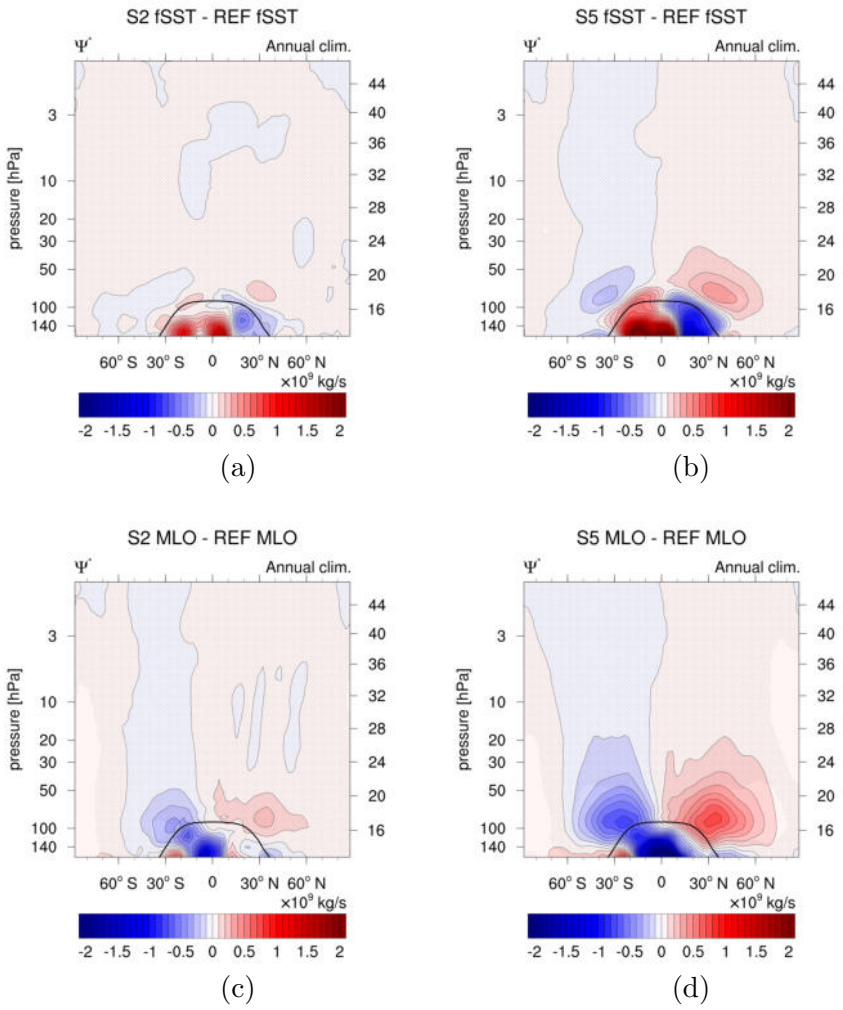

Figure 2. Absolute differences of the annual zonal mean residual streamfunction between the sensitivity simulations (a) S2 fSST, (b) S5 fSST, (c) S2 MLO, (d) S5 MLO compared to their respective reference in 10^9 kg s^{-1}. Non-stippled areas are significant on the 95 % confidence level according to a two sided Welch's test. The solid black line indicates the climatological tropopause height of REF MLO.

3.3 Influence of interactive SSTs

3.3.1 Chemical composition

Winterstein et al. (2019) analysed the quasi-instantaneous impact of doubled and fivefold CH_4 mixing ratios on the chemical composition of the atmosphere. In this section we investigate ~~how tropospheric warming and associated climate feedbacks (see Sect. 3.2) modify these rapid adjustment patterns. For this purpose the difference patterns of the sensitivity simulationsare compared to those of the fSST simulations~~the respective slow feedbacks that are assessed as the difference between the full

response (as simulated in the MLO simulations) and the rapid adjustments (as simulated in the fSST simulations) and therefore visualized as differences of the differences.

Tropospheric CH_4 lifetime and OH

~~Winterstein et al. (2019) found a near-linear prolongation of the tropospheric lifetime, related to the~~ The oxidation with OH ~~, with increasing scaling factor of the mixing ratio. The -oxidation~~ is the most important sink of CH_4 in the troposphere (e.g., Saunois et al., 2016a). The amount of oxidised CH_4 affects the OH mixing ~~ratio~~ ratios as the reaction consumes OH, which in turn feeds back on the atmospheric CH_4 lifetime. In this study, consistent with Winterstein et al. (2019), the CH_4 lifetime is calculated according to Jöckel et al. (2016) as

$$\tau_{CH_4} = \frac{\sum\limits_{b \in B} m_{CH_4}}{\sum\limits_{b \in B} k_{CH_4+OH}(T) \cdot c_{air}(T,p,q) \cdot x_{OH} \cdot m_{CH_4}}, \quad (1)$$

with m_{CH_4} being the mass of CH_4 in ~~kg~~[kg], $k_{CH_4+OH}(T)$ the temperature dependent reaction rate coefficient of the reaction $CH_4 + OH \rightarrow$ products in [cm^3 s^{-1}], c_{air} the concentration of air in [~~mol~~ cm^{-3}] and x_{OH} the mole fraction of OH in [mol mol^{-1}] in all grid boxes b $\in$ B. B is the region, for which the lifetime should be calculated, e.g. all grid boxes below the tropopause for the mean tropospheric lifetime. For the CH_4 lifetime calculation a climatological tropopause, defined as $tp_{clim} = 300\,hPa - 215\,hPa \cdot \cos^2(\phi)$, with ϕ being the latitude in degree north, is used as recommended by Lawrence et al. (2001) .

Figure 3 shows the mean tropospheric CH_4 lifetime of the MLO experiments, together with the fSST experiments, dependent on the CH_4 scaling factor, i.e. 1 for the reference simulations, 2 for the experiments with 2×CH_4, and 5 for those with 5×CH_4. An almost linear relationship between the mean tropospheric CH_4 lifetime and the CH_4 scaling factor is present also in the MLO sensitivity simulations. The lifetime increase is, however, reduced by 0.30 a (increase by 2.03 a instead of 2.33 a) and 1.17 a (increase by 6.37 a instead of 7.54 a) in the MLO set-up compared to fSST when doubling and fivefolding CH_4, respectively. This weaker increase is in line with a weaker decrease of tropospheric OH in the MLO sensitivity simulations compared to fSST as obvious from Fig. ~~??, which shows~~ 4 (c) and (d), which show the difference between the OH response in the MLO and in the fSST sensitivity simulations~~(see Fig. 4 in Winterstein et al., 2019 and Fig. S7 for the respective response patterns of in the fSST and the MLO simulations, respectively).~~ . In the troposphere ~~the difference between the response in the and in the fSST experiments~~ this difference is hardly significant anywhere for the 2×CH_4 experiments, whereas it is significant in the tropics for 5×CH_4. The weaker decrease of tropospheric OH in both MLO simulations is related to more strongly enhanced OH precursors (H_2O and O_3) in the troposphere in the MLO compared to the fSST sensitivity simulations, as will be discussed below. Additionally, the tropospheric warming in the MLO sensitivity simulations results in a faster CH_4 oxidation as its reaction rate increases with temperature. The isolated effect of the temperature dependent reaction rate is indicated by the blue squares in Fig. 3. They show the CH_4 lifetime corresponding to REF MLO conditions, except for the reaction rate coefficient that was calculated with temperatures corresponding to 2× and 5× CH_4.

Table 2. Increase factors of the global mean CH_4 surface fluxes, which correspond to increases of the CH_4 mixing ratios by factors of 2 or 5, respectively. The values after the $\pm$ sign are the 95 % confidence intervals of the mean calculated using Taylor expansion and assuming S2/S5 and REF fluxes to be uncorrelated as $\pm\, t_{\frac{\alpha}{2},\mathrm{df}} \cdot \frac{\overline{x}}{\overline{y}} \cdot \sqrt{\frac{s_x^2}{N_x \cdot \overline{x}} + \frac{s_y^2}{N_y \cdot \overline{y}}}$ with the mean values of the S2/S5 and REF fluxes $\overline{x}$ and $\overline{y}$, respectively, interannual standard deviations s_x and s_y, number of analysed years N_x and N_y, $\alpha = 0.05$, and the degrees of freedom $df = (\frac{s_x^2}{N_x} + \frac{s_y^2}{N_y}) \cdot (\frac{(\frac{s_x^2}{N_x})^2}{N_x - 1} + \frac{(\frac{s_y^2}{N_y})^2}{N_y - 1})^{-1}$.

	fSST	MLO
S2	1.58 ± 0.00	1.61 ± 0.01
S5	2.75 ± 0.01	2.91 ± 0.01

Voulgarakis et al. (2013) compared the CH_4 lifetime increase of two simulations, one with the full RCP8.5 climate change signal of the year 2100 with respect to 2000, and one with CH_4 concentrations corresponding to 2100 RCP8.5 levels, but climate conditions of the year 2000. They identified a weaker increase of the CH_4 lifetime with tropospheric warming as well. Their difference is larger than the difference between the S2 fSST and S2 MLO lifetime responses, even though the CH_4 increase simulated by Voulgarakis et al. (2013) is of the same order of magnitude as in S2 fSST and S2 MLO, since the RCP8.5 scenario projects a doubling of the 2010 CH_4 mixing ratios at the end of the century. However, the tropospheric warming in the RCP8.5 scenario is stronger because it includes the effects of all GHGs~~and not only the~~, as opposed to the isolated effect of CH_4 ~~. This can explain the larger offset of the~~ in our experiments. Additional warming induced by other GHGs, in particular CO_2, would drive H_2O and O_3 increases as well. Therefore, the reduction in OH driven by CH_4 ~~lifetime response reported by Voulgarakis et al. (2013)~~ increases in our experiments is expected to be more strongly offset under a simultaneously active CO_2 forcing.

Please recall that we prescribe the CH_4 mixing ratios at the lower boundary using Newtonian relaxation. It is important to note that the prolongation of the tropospheric CH_4 lifetime causes the corresponding CH_4 fluxes at the lower boundary to not scale equally with the mixing ratio increase, but to increase by a smaller factor. Increasing the CH_4 surface mixing ratio by a factor of 2 (5) corresponds to an increase of the CH_4 surface fluxes by a factor of 1.61 ± 0.01 (2.91 ± 0.01) in the MLO simulations, and by a factor of 1.58 ± 0.00 (2.75 ± 0.01) in the fSST simulations (see Tab. 2). The larger increase factors in the MLO sensitivity simulations are in line with the reduced prolongation of the tropospheric CH_4 lifetime compared to the fSST experiments. The fact that the increase in emission fluxes is less than a factor of 2 or 5 suggests that enhanced CH_4 emissions would likewise scale the mixing ratio by a larger factor than the corresponding increase factor of the emissions. The CH_4 surface fluxes that result from the nudging of the mixing ratio towards zonally averaged CH_4 fields are not realistic in terms of spatial distribution, however.

Non-linearities of CH_4 increase

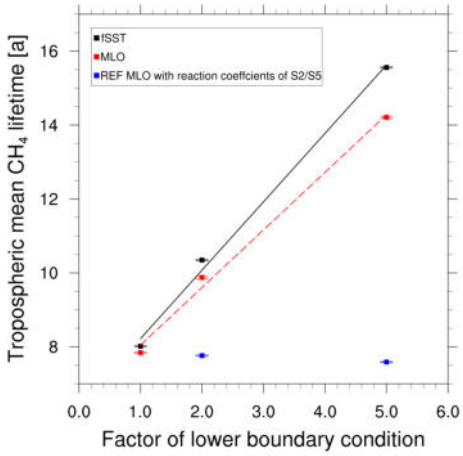

Figure 3. Mean tropospheric CH_4 lifetime with respect to the oxidation with OH versus the scaling factor of the lower boundary CH_4, i.e. 1 for REF, 2 for S2, 5 for S5 for the MLO (red, dashed) and the fSST (black, solid) simulations. In addition, the isolated effect of the temperature dependent reaction rate is shown for the MLO experiments (blue squares). The vertical lines indicate the 95 % confidence intervals based on annual mean values of the CH_4 tropospheric lifetime.

~~Winterstein et al. (2019) investigated whether the increase of atmospheric follows the doubling or fivefolding for fSST conditions~~ ~~linearly. Tropospheric is largely controlled by the nudging at the lower boundary through mixing and responds linearly to the increase. However, the increase between 50 and 1 hPa has found to be smaller than a strictly linear relation would predict. This indicates enhanced chemical depletion in the stratosphere due to changes in the chemical composition.~~ Fig. ~~??~~ 5 shows the relative ~~difference~~ differences between the annual zonal mean CH_4 of S2 MLO (S5 MLO) and $2\times$ ($5\times$) the zonal mean CH_4 of REF MLO. The doubling or fivefolding of the reference CH_4 serves to emphasize regions where the increase factor of the CH_4 mixing ratio deviates from 2 or 5, respectively. The response of tropospheric CH_4 is marginally larger than a linear increase in both MLO experiments. This is in line with the response of tropospheric CH_4 in the fSST simulations. Tropospheric CH_4 is largely controlled by the nudging at the lower boundary through mixing and is, therefore, prevented to adjust to the lifetime increase as discussed above. The slightly positive values in Fig. 5 indicate a small residual of this effect. As for the fSST simulations, the CH_4 increase ~~in the extratropical stratosphere is weaker than a linear increase in both sensitivity simulations.~~ ~~The non-linearity~~ between 50 and 1 hPa is smaller than the factors of 2 or 5, respectively. This effect is less pronounced in the two MLO sensitivity experiments compared to the respective fSST experiments (compare with Fig. 3 in Winterstein et al., 2019) suggesting that the chemical depletion of CH_4 is enhanced in the MLO experiments as well, however, less strongly than in the fSST experiments.

Another aspect to note in Fig. ~~??~~ 5 is the more than $2\times$ or $5\times CH_4$ increase in the lowermost tropical stratosphere~~for S5 MLO~~. This feature indicates enhanced tropical upwelling, which leads to larger CH_4 mixing ratios in the tropical lower stratosphere.

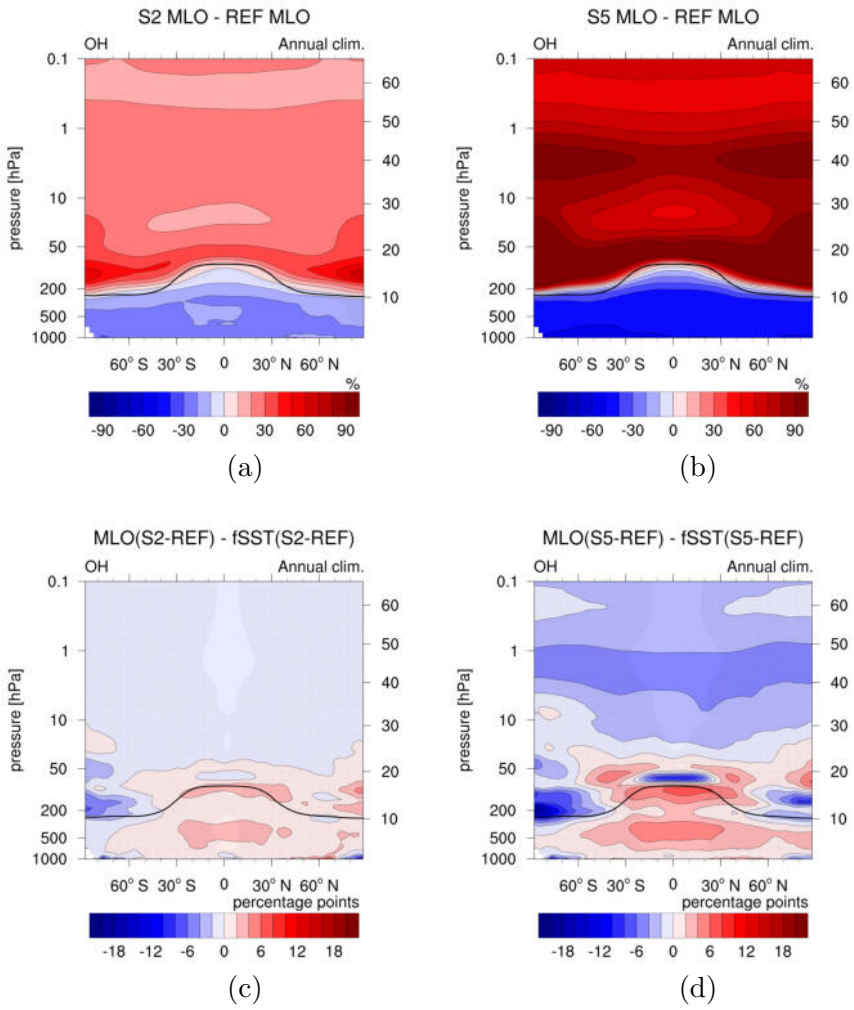

Figure 4. Upper row: Relative differences between the annual zonal mean OH mixing ratios of the sensitivity simulations (a) S2 MLO and (b) S5 MLO and REF MLO in %. Lower row: Differences between the OH response to enhanced CH_4 in the MLO and fSST set-ups in percentage points. To calculate the ~~difference~~ latter the relative changes of (c) S2 fSST and (~~left~~d) ~~and~~ S5 fSST ~~(right)~~ are subtracted from the relative changes of S2 MLO and S5 MLO, respectively. Non-stippled areas are significant on the 95 % confidence level according to a two sided Welch's test. The solid black line indicates the climatological tropopause height of REF MLO.

~~This feature~~ It is more pronounced in ~~S5~~ the MLO than in ~~S5 fSST~~ the fSST experiments, in line with the more pronounced changes of tropical upwelling in the MLO set-up as discussed in Sect. 3.2. The average deviation from 2× or 5×CH_4 for a region in the tropical lower stratosphere (30°S–30°N, 70–20 hPa) is 0.16 % for S2 fSST, 0.37 % for S2 MLO, 0.23 % for S5 fSST, and 1.31 % for S5 MLO. Furthermore, strengthening of the BDC transports CH_4 more efficiently to higher altitudes leading to higher CH_4 mixing ratios there as well. This can be one explanation for the weaker deviation from a linear CH_4 increase in the MLO compared to the fSST simulations. Another explanation, as already stated, is that the chemical depletion

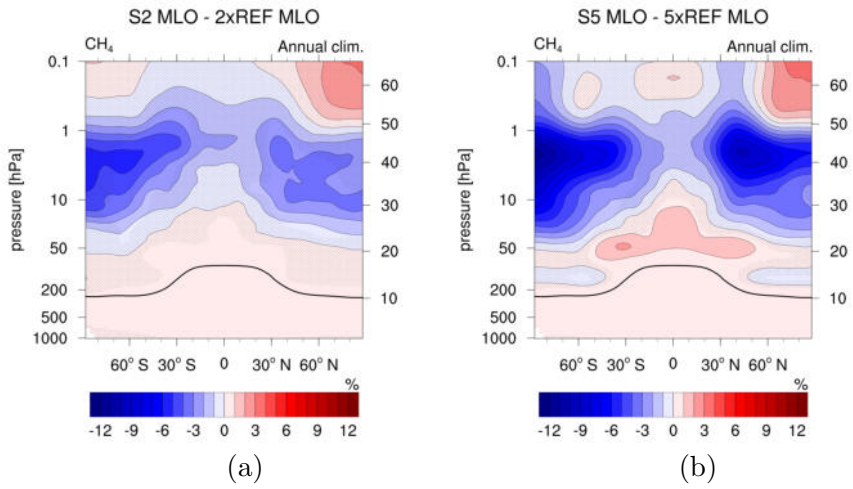

Figure 5. Relative differences between the annual zonal mean CH_4 of the sensitivity simulations (a) S2 MLO and 2× REF MLO and (~~left~~b) ~~and~~ S5 MLO and 5× REF MLO ~~(right)~~ in %. Non-stippled areas are significant on the 95 % confidence level according to a two sided Welch's test. The solid black line indicates the climatological tropopause height of REF MLO.

of CH_4 is less strongly enhanced in the MLO sensitivity simulations compared to fSST. We therefore discuss differences of the response of OH, the most important sink partner of CH_4, in the next paragraph.

Stratospheric OH mixing ratios increase in both simulation set-ups (fSST and MLO) at the order of 30 % for 2×CH_4 and 60 %–80 % for 5×CH_4 (see Fig. 4 in Winterstein et al. (2019) for fSST and Fig. 4 (a) and (b) for MLO). ~~As shown by Winterstein et al. (2019) , precursors (and) in the stratosphere are also affected by the increase.~~ The OH increase in the stratosphere is weaker in the MLO simulations compared to the fSST simulations (see Fig. ~~??)~~ 4 (c) and (d)). The differences are, however, small compared to the total increase of OH and mainly not significant. The difference between the two 5×CH_4 experiments reaches up to 5 percentage points (p.p.) in the middle stratosphere. The weaker increases of OH are presumably connected to weaker increases of SWV in the MLO simulations. The considerably weaker OH increase above the tropical tropopause in S5 MLO with respect to S5 fSST is possibly associated with a stronger O_3 decrease in this area in S5 MLO. Both, changes in SWV and O_3, will be discussed below. The weaker OH increases in the MLO sensitivity experiments with respect to fSST are in line with the smaller deviations from a linear doubling or fivefolding of the CH_4 mixing ratio in the stratosphere (see Fig. ~~??~~5). We conclude that the strengthening of the CH_4 oxidation resulting from increases of the OH mixing ratio is weaker in the MLO experiments, but still present.

Water vapour

~~is a precursor of and its abundance is also influenced by mixing ratios.~~ Winterstein et al. (2019) reported a steady increase of SWV with height for the fSST experiments as an outcome of the enhanced CH_4 ~~doubling and fivefolding experiments with prescribed and . Figure ?? shows the difference of the~~ depletion as discussed in the previous paragraph, whereas tropospheric

H_2O ~~response between the and the fSST simulations (see Fig. 5 in Winterstein et al., 2019 and Fig. S8 for the respective response patterns of in the fSST and the MLO simulations, respectively). As the saturation vapour pressure increases with temperature, the~~ remained largely unaffected. The warming of the troposphere in the MLO simulations consistently leads to ~~a stronger~~ an increase of the ~~tropospheric~~ H_2O mixing ~~ratio in comparison with the respective fSST simulation.~~ratios also in the troposphere as evident from Fig. 6. The maximum difference in tropospheric H_2O response between MLO and fSST can be found in the upper tropical troposphere and extratropical lowermost stratosphere and reaches 11 p.p. (35 p.p.) for the 2× (5×) CH_4 experiments.

In the middle and upper stratosphere, the H_2O increase is about 5 p.p. (15 p.p.) weaker in the S2 MLO (S5 MLO) sensitivity simulation compared to S2 fSST (S5 fSST). This reduction is significant, but small compared to the relative increase of SWV of around 50 % for both 2×CH_4, and 250 % for both 5×CH_4 experiments. The amount of tropospheric H_2O transported into the stratosphere is largely determined by the cold point temperature (CPT) (e.g., Randel and Park, 2019). Furthermore, the oxidation of CH_4 is an important in-situ source of SWV (Hein et al., 2001; Rohs et al., 2006; Frank et al., 2018). The SWV mixing ratio at a given location and time can be approximated as the sum of these two terms ~~(Austin et al., 2007; Revell et al., 2016) .~~ following Austin et al. (2007); Revell et al. (2016) as

$$H_2O = H_2O_{\text{entry}} + H_2O_{\text{CH4}}. \quad (2)$$

We calculate the amount of tropospheric H_2O entering the stratosphere as the tropical (10°~~N–10~~S–10°~~S~~N) mean H_2O mixing ratio at 70 hPa following Revell et al. (2016). The H_2O entry mixing ratio increases by ~~about 10~~9.08 % (~~40) in the doubling (fivefolding) experiments (both MLOand fSST) . The relative increases are insignificantly higher in both experiments compared to the respective fSSTexperiment~~0.14 ppm) in S2 fSST, 9.77 % (0.17 ppm) in S2 MLO, 38.53 % (0.57 ppm) in S5 fSST, and 38.86 % (0.68 ppm) in S5 MLO. Furthermore, the zonal mean tropical CPT increases in all sensitivity simulations (see Fig. ~~S9). The magnitude and the latitude dependence~~ S7). Though differences exist between the reference CPT in MLO und fSST, the magnitude and latitudinal structure of the CPT changes are very similar for both doubling and both fivefolding experiments~~, although slightly~~ . They are also a bit larger for the ~~experiments~~ MLO experiments (again consistent for the S2 and S5 case), in line with the ~~changes~~ response of the H_2O entry mixing ~~ratio~~ratios. Changes of the amount of tropospheric H_2O entering the stratosphere can therefore not explain the ~~differences in the response between and fSST in the middle and upper stratosphere. The increases of the entry mixing ratio and the are both slightly stronger in the experiments and would therefore suggest a stronger~~ weaker increase of SWV in the ~~experiments . On the contrary, the increases of are weaker~~ MLO experiments compared to fSST in the middle and upper stratosphere~~in the experiments compared to fSST. The contribution of the~~ .

To illustrate the effect of CH_4 oxidation on the SWV ~~can explain these weaker increases of in the MLO experiments. The~~ response, Fig. S8 shows the response of H_2O from CH_4 oxidation estimated using Eq. 2. As discussed in the previous paragraph, the strengthening of the CH_4 oxidation in the stratosphere is weaker in the MLO experiments~~resulting likewise~~ . This results in a weaker increase of SWV produced by CH_4 oxidation ~~.~~ in the middle and upper stratosphere (see Fig. S8 (c) and (d)) and can explain the difference of SWV response between MLO and fSST as shown in Fig. 6 (c) and (d).

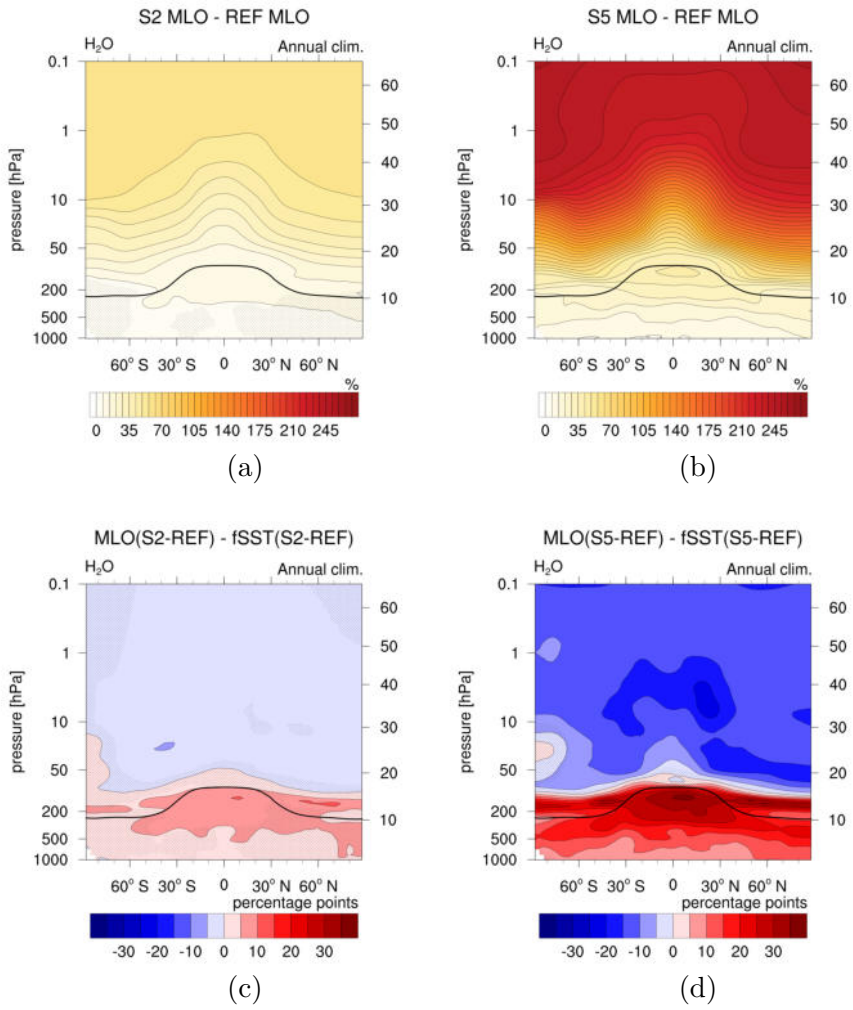

Figure 6. Upper row: Relative differences between the annual zonal mean H_2O mixing ratios of the sensitivity simulations (a) S2 MLO and (b) S5 MLO and REF MLO in %. Lower row: Differences between the H_2O response to enhanced CH_4 in the MLO and fSST set-ups in percentage points. To calculate the ~~difference~~ latter the relative changes of (c) S2 fSST and (~~left~~d) ~~and~~ S5 fSST ~~(right)~~ are subtracted from the relative changes of S2 MLO and S5 MLO, respectively. Non-stippled areas are significant on the 95 % confidence level according to a two sided Welch's test. The solid black line indicates the climatological tropopause height of REF MLO.

What remains to be explained is the reason for the weaker strengthening of the CH_4 oxidation in the MLO setup compared to fSST. Strengthened tropical upwelling as shown in Sect. 3.2 transports CH_4 into the stratosphere more efficiently and would be expected to lead to higher rates of the CH_4 oxidation (Austin et al., 2007). However, as the strengthening of the CH_4 oxidation is weaker in the MLO experiments, CH_4 itself seems not to be the limiting factor here. The abundance of SWV feeds back on OH and therefore also on the efficiency of the CH_4 oxidation. However, the increase of SWV seems to be rather a result of the

strengthened CH_4 oxidation here, as the increase of H_2O entering the stratosphere is higher in the MLO experiments compared to fSST.

Ozone

The other important precursor of OH is O_3, the abundance of which is also influenced by CH_4. The stratospheric O_3 response pattern in the MLO experiments, namely O_3 reduction in the lowermost tropical stratosphere, O_3 increase up to approximately 2 hPa, and O_3 decrease above, is qualitatively consistent with the fSST simulations (compare Fig. 7 in Winterstein et al., 2019 and Fig. ~~S10)~~ 7 (a) and (b)). Winterstein et al. (2019) gave a detailed explanation of the processes leading to the resulting O_3 pattern that is also valid for the MLO simulations. As the O_3 catalytic depletion cycles are less efficient at lower temperatures radiative cooling in the stratosphere results in increased O_3 mixing ratios in the middle stratosphere (between 50 and 5 hPa). Additionally, increased abundances of H_2O favor the depletion of excited oxygen ($O(^1D)$), likewise reducing the sink of O_3 and favoring increases of the O_3 abundance. Reduced O_3 mixing ratios in the lowermost tropical stratosphere indicate enhanced tropical upwelling of O_3 poor air from the troposphere into the stratosphere. Above 2 hPa, increases of OH lead to enhanced depletion of O_3 resulting in reduced O_3 mixing ratios.

When subtracting the fSST response from the MLO response, the extra effect of tropospheric warming becomes apparent. The resulting patterns for S2 and S5 are shown in Fig. ~~??~~7 (c) and (d). A dominant feature is the stronger decrease of O_3 in the lowermost tropical stratosphere in S5 MLO compared to S5 fSST of up to ~~18~~18.39 p.p.. The average difference between S5 MLO and S5 fSST for a region in the tropical lower stratosphere (30°S–30°N, 100–20 hPa) is 6.33 p.p.. This difference also exists between the S2 simulations, albeit weaker (~~4~~with a maximum difference of 4.68 p.p. and an average difference of 1.67 p.p.). The more strongly decreasing O_3 mixing ratios in MLO indicate that the transport of O_3 poor air from the troposphere into the stratosphere is intensified in the MLO simulations. The increases of O_3 in the southern polar middle stratosphere in S2 MLO, and in both polar regions in S5 MLO are more pronounced with respect to the respective fSST experiment. This indicates more strongly enhanced meridional transport in the MLO experiments. Both patterns are in line with the strengthening of the residual mean circulation as discussed in Sect. 3.2.

In the tropospheric O_3 response pattern (shown in Fig. ~~S10)~~ 7 (a) and (b)) any O_3 feedback from tropospheric warming is superimposed by chemical influences of CH_4. Therefore, the pattern is fundamentally different from O_3 changes in global warming simulations driven by CO_2 increases (see Fig. 1 (a) in Dietmüller et al., 2014, Fig. 3 (a) in Nowack et al., 2018, and Fig. 1 (a) - (c) in Chiodo and Polvani, 2019), where direct chemical impacts are weak. However, if the O_3 response to slow climate feedbacks induced by enhanced CH_4 is separated from rapid adjustments (Fig. ~~??)~~ 7 (c) and (d)), a similar pattern to the O_3 response induced by enhanced CO_2 arises. An exception is the increase of O_3 above 30 hPa that results from a slower chemical depletion of O_3 caused by stratospheric radiative cooling (Dietmüller et al., 2014), which develops on the timescale of rapid radiative adjustments. A deceleration of the chemical O_3 destruction in the middle stratosphere is also present in the CH_4~~driven~~ -driven experiments resulting mainly from radiative cooling induced by adjustments of SWV and O_3 (see Fig. 8 (e) and (f) in Winterstein et al., 2019), but cancels out in Fig. ~~??~~7 (c) and (d).

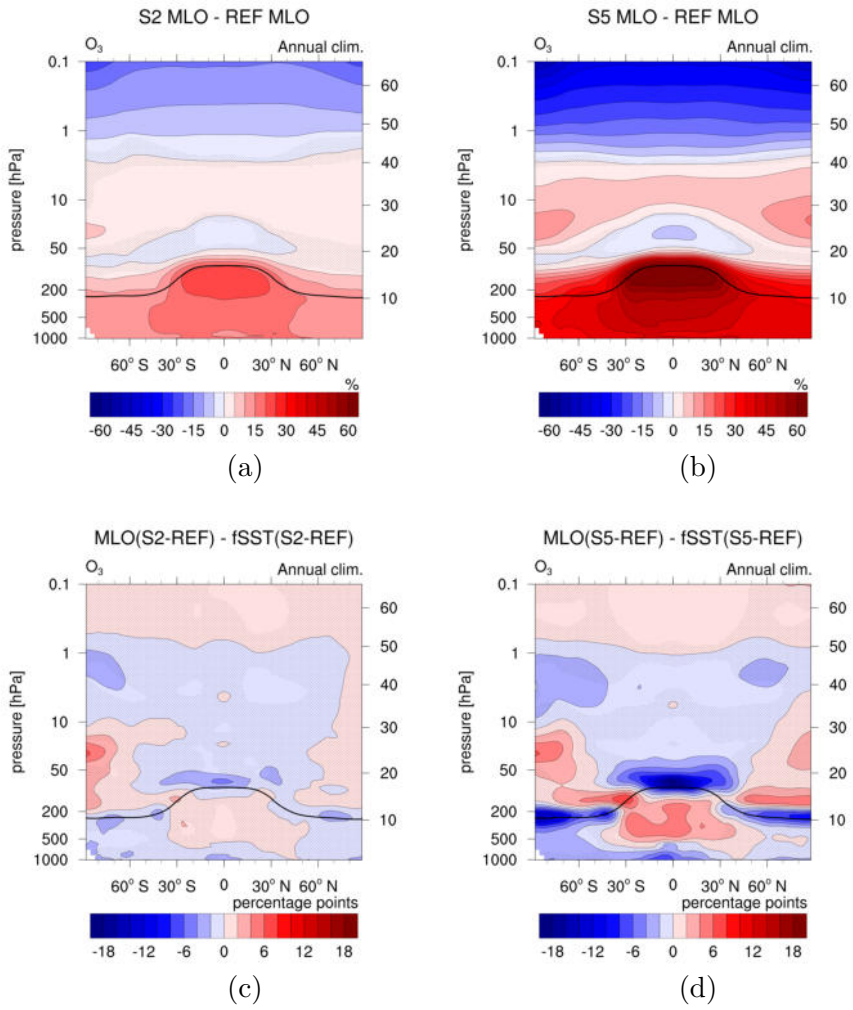

Figure 7. Upper row: Relative differences between the annual zonal mean O_3 mixing ratios of the sensitivity simulations (a) S2 MLO and (b) S5 MLO and REF MLO in %. Lower row: Differences between the O_3 response to enhanced CH_4 in the MLO and fSST set-ups in percentage points. To calculate the ~~difference~~ latter the relative changes of (c) S2 fSST and (~~left~~d) ~~and~~ S5 fSST ~~(right)~~ are subtracted from the relative changes of S2 MLO and S5 MLO, respectively. Non-stippled areas are significant on the 95 % confidence level according to a two sided Welch's test. The solid black line indicates the climatological tropopause height of ~~the~~ REF MLO.

3.3.2 Radiative impact, surface temperature response and climate sensitivity

In Winterstein et al. (2019) the total RI has been separated into the individual contributions of the species CH_4, SWV, and O_3, an analysis we extend hereafter to the MLO simulations. Note, that we adopt the definition of Winterstein et al. (2019) concerning the RI, which indicates the radiative flux imbalance between the sensitivity and the reference simulation.

In Table 3 we summarize the RI of the most important species in both the fSST and the MLO simulations. The individual contributions to the RI have been calculated with the submodel RAD (Dietmüller et al., 2016) in separate simulations (S2 fSST*, S5 fSST*, S2 MLO* and S5 MLO*; see Sect. 2). We further separate the H_2O and O_3 contribution into tropospheric and stratospheric RI, respectively. The RIs of CH_4 and O_3 show only small differences between fSST and MLO. This implies that SST-driven climate feedbacks on these constituents do not substantially alter their RI contribution in our simulation set-up. As expected, the RI of tropospheric H_2O increases substantially~~(from 0.08 ± 0.05 to 0.72 ± 0.04 for $2\times$ and from 0.30 ± 0.06 to 2.23 ± 0.06 for $5\times$)~~. The RI of stratospheric H_2O increases as well, which is mostly influenced by the increase in SWV in the lowermost stratosphere due to transport of moist air from the tropical troposphere into the stratosphere (see Fig. **??**6).

The global mean surface temperature responses in the MLO experiments for $2\times$ and $5\times CH_4$ are 0.42 ± 0.05 K and 1.28 ± 0.04 K, respectively. ~~Under the~~ The forcing strengths of $2\times$ and $5\times CH_4$ turn out too small to robustly quantify the corresponding climate sensitivity parameters λ with a sensitivity analysis of the entire transient data following Gregory et al. (2004) . Therefore, we calculate λ, under the reasonable assumption that the total RIs from the fSST experiments represent the corresponding ERFs with chemical rapid adjustments included (Winterstein et al., 2019), ~~we calculate the climate sensitivity parameters λ~~ as 0.61 ± 0.17 K W^{-1} m^2 and 0.72 ± 0.07 K W^{-1} m^2, respectively. The estimate of λ corresponding to $5\times CH_4$ compares well with the climate sensitivity parameter λ_{adj} of 0.73 K W^{-1} m^2 from Rieger et al. (2017) corresponding to a $1.2\times CO_2$ experiment with EMAC with a radiative forcing (RF) of 1.06 Watt per square meter (W m^{-2}), which is comparable to the RIs in the present experiments. The agreement of the climate sensitivity parameters for CH_4- and CO_2-forcing suggests an efficacy of CH_4 ERF close to one. The estimate of λ for $2\times CH_4$ is smaller than the value from Rieger et al. (2017), but the difference is insignificant as a consequence of large statistical uncertainty.

In a recent multimodel comparison, the multimodel mean efficacy of CH_4 was found to be smaller than one, however, with a large intermodel spread ranging from 0.56 to 1.15 (Richardson et al., 2019). Modak et al. (2018) found a CH_4 efficacy of 0.81 for CH_4 for a simulation with a CH_4 increase comparable to S5. They identified CH_4 shortwave (SW) absorption and related warming of the lower stratosphere and upper troposphere as reason for the smaller efficacy of CH_4. Our simulation set-up does not account for SW absorption of CH_4. The climate sensitivity and efficacy estimates of Modak et al. (2018) and Richardson et al. (2019) do not include chemical feedbacks of O_3 and SWV induced by CH_4. They also do not provide a robust indication that the CH_4 efficacy is significantly larger or smaller than unity in their framework, as the inter-model spread reported by (Richardson et al., 2019) is so large. Estimating a reasonable climate sensitivity value from our simulations in an interactive chemistry framework, requires that rapid adjustments from SWV and O_3 are included in the effective CH_4 forcing. If this is done, these simulations do not point at a significant climate sensitivity deviation from the CO_2 behavior either.

3.3.3 Radiatively and dynamically driven atmospheric temperature response

The two lower panels in Fig. ~~?? shows~~ 1 show the differences of temperature response between the MLO and the fSST simulations. As expected, tropospheric warming is significantly stronger in the MLO experiments, since the tropospheric temperature change is largely suppressed in the simulations with prescribed SSTs and SICs. In the stratosphere, radiatively and dynamically driven effects contribute to differences in the temperature change patterns between MLO and fSST, as will

Table 3. An estimation of individual RI contributions in [W m^{-2}] of the changes in the chemical species CH_4, H_2O and O_3. Values are calculated using the RAD submodel (Dietmüller et al., 2016) in separate simulations (S2 fSST*, S5 fSST*, S2 MLO* and S5 MLO*, see Sect. 2) using 20 years climatologies of the individual species from the corresponding reference and sensitivity simulation experiments fSST and MLO. The lower part shows the global mean 2 m air temperature changes of S2 MLO and S5 MLO with respect to REF MLO and the total RIs of S2 fSST and S5 fSST. From these temperature changes and total RIs the climate sensitivity parameter λ is calculated as $\lambda = \Delta T_{MLO}$ / total RI_{fSST}.

Simulation	CH_4	trop. H_2O	strat. H_2O	total H_2O	trop. O_3	strat. O_3	total O_3
S2 fSST*	0.23 ± 0.01	0.08 ± 0.05	0.15 ± 0.00	0.24 ± 0.05	0.22 ± 0.01	0.06 ± 0.01	0.27 ± 0.02
S5 fSST*	0.51 ± 0.02	0.30 ± 0.06	0.55 ± 0.01	0.85 ± 0.06	0.56 ± 0.02	0.20 ± 0.02	0.76 ± 0.02
S2 MLO*	0.23 ± 0.01	0.72 ± 0.04	0.19 ± 0.00	0.91 ± 0.04	0.22 ± 0.01	0.06 ± 0.00	0.28 ± 0.01
S5 MLO*	0.52 ± 0.02	2.23 ± 0.06	0.65 ± 0.01	2.87 ± 0.07	0.57 ± 0.02	0.19 ± 0.01	0.76 ± 0.02
	ΔT_{MLO} [K]	total RI_{fSST} [W m^{-2}]	λ [K W^{-1} m^2]				
S2	0.42 ± 0.05	0.69 ± 0.16	0.61 ± 0.17				
S5	1.28 ± 0.04	1.79 ± 0.17	0.72 ± 0.07				

The values after the $\pm$ sign are the 95 % confidence intervals of the mean.

For λ the confidence intervals are calculated using Taylor expansion and assuming ΔT_{MLO} and total RI_{fSST} to be uncorrelated as $\pm\, t_{\frac{\alpha}{2},df} \cdot \frac{\overline{x}}{\overline{y}} \cdot \sqrt{\frac{s_x^2}{N_x \cdot \overline{x}} + \frac{s_y^2}{N_y \cdot \overline{y}}}$ with the mean values of ΔT_{MLO} and total RI_{fSST} $\overline{x}$ and $\overline{y}$, respectively, interannual standard deviations s_x and s_y, number of analysed years N_x and N_y, $\alpha = 0.05$, and the degrees of freedom $df = (\frac{s_x^2}{N_x} + \frac{s_y^2}{N_y}) \cdot (\frac{(\frac{s_x^2}{N_x})^2}{N_x - 1} + \frac{(\frac{s_y^2}{N_y})^2}{N_y - 1})^{-1}$.

be shown in the following. Note again that changes in the chemical composition resulting from a change in circulation (i.e. transport) are included in the radiatively driven effects by our definition.

Following Winterstein et al. (2019) we calculate the stratospheric adjusted temperature response ΔT_{adj} to changes in CH_4, tropospheric and stratospheric H_2O, and tropospheric and stratospheric O_3, as well as their individual contributions, for S2 MLO and S5 MLO (see Fig. ~~S11~~ S9 for simulation S2 MLO and Fig. 8 for simulation S5 MLO). ΔT_{adj} represents the temperature response induced by composition changes of radiatively active gases (Stuber et al., 2001) . The difference of ~~adjusted stratospheric temperature response~~ ΔT_{adj} between S5 MLO and S5 fSST is shown in Fig. 9 (for S2 see Fig. ~~S12~~S10). This difference is small for CH_4 and tropospheric O_3 (see Fig. 9 (b) and (g)). Figure~~9~~ 9 (d) confirms the stratospheric radiative cooling effect of increased humidity in the troposphere in S5 MLO, although the effect is quantitatively small. The adjusted stratospheric temperature response pattern induced by SWV in S5 MLO is similar to S5 fSST. However, the stronger increases of SWV in S5 MLO result in more pronounced cooling in the lowermost stratosphere, whereas the reduced increases above consistently result in reduced cooling (see Fig. 9 (e)). The stronger decrease of O_3 in the tropical lower stratosphere in S5 MLO (see Fig. ~~??~~7) leads to stronger cooling in this region as shown in Fig. 9 (h). These results also apply qualitatively to the comparison of S2 MLO and S2 fSST (see Fig. ~~S12~~S10), but the magnitude of the differences is smaller. The effects from SWV and stratospheric O_3 dominate the differences of ~~stratospheric adjusted temperature~~ ΔT_{adj} between S5 MLO and

S5 fSST (compare Fig. 9 (a)). In addition, the resulting more pronounced cooling in the lowermost stratosphere in the MLO simulations is apparent in the difference between the overall temperature responses of MLO and fSST in Fig. ??1 (c) and (d).

By calculating the difference between the total temperature response in the regular simulations ΔT and the sum of the individual contributions of CH_4, H_2O and O_3 to the adjusted stratospheric temperatures ~~,~~(ΔT_{adj}^{total}, see Fig. 8 (a) and Fig. S9 (a)), we attempt to identify the dynamical effect ($\Delta\tilde{T}_{dyn.}$) in the stratospheric temperature response as

~~$\Delta\tilde{T}_{dyn.} = \Delta T(SX\text{-}REF) - \Delta T_{addst}(SX^*\text{-}REF^*)$~~

$$\Delta\tilde{T}_{dyn.} = \Delta T(SX\text{-}REF) - \Delta T_{adj}^{total}(SX^*\text{-}REF^*)$$

with X being either 2 or 5. A similar approach was, for example, used by Rosier and Shine (2000) and Schnadt et al. (2002) to distinguish between the radiative impact of trace gases and dynamical contributions to the total temperature response.

Fig. 10 shows the annual mean of $\Delta\tilde{T}_{dyn.}$ for all four sensitivity simulations. It is mostly not significant for S2 fSST and S5 fSST in the stratosphere suggesting that dynamical effects play a minor role in the temperature response in these simulations as already indicated by Winterstein et al. (2019). However, immediately above the tropical tropopause centered at the equator $\Delta\tilde{T}_{dyn.}$ indicates warming for both, S2 fSST and S5 fSST. In austral winter (JJA), $\Delta\tilde{T}_{dyn.}$ shows significant cooling in the southern polar stratosphere for S2 fSST and S5 fSST. The cooling extends into austral spring (SON), but gradually weakens as time proceeds (see Fig. ~~S15~~ S13 and Fig. ~~S16~~S14). These temperature changes can be associated to the strengthening of the SH stratospheric winter polar vortex (see Fig. ~~S18~~S16), which leads to enhanced isolation of airmasses and stronger cooling. The stratospheric polar vortex in boreal winter DJF accelerates in both fSST sensitivity simulations as well (see Fig. ~~S17~~S15).

The pattern of $\Delta\tilde{T}_{dyn.}$ for S5 MLO (Fig. 10 (d)) displays a near-symmetrical behavior around the equator. It comprises of two warming patches in the lower stratosphere - unlike S5 fSST not centered at the equator, but at around 30°S or 30°N -, as well as cooling in the tropics and warming in the extratropics in the middle stratosphere. The warming patches in the lower stratosphere are present in all seasons, whereas the pattern of cooling in the tropics and warming in the extratropics above is shifted to the respective winter hemisphere (compare Fig. ~~S13~~ S11 and Fig. ~~S15~~S13). For S2 MLO, the warming patches in the lower stratosphere are also present in the pattern of $\Delta\tilde{T}_{dyn.}$. Apart from that, the annual mean $\Delta\tilde{T}_{dyn.}$ is mostly not significant for S2 MLO. However, the pattern of cooling in the tropics and warming in the extratropics is indicated in boreal autumn (SON) and winter (DJF) for S2 MLO as well.

We associate the main component of the $\Delta\tilde{T}_{dyn.}$ pattern of the MLO experiments with the strengthening of the BDC as discussed in Sect. 3.2. Strengthened downwelling in the subtropical and extratropical lower stratosphere results in adiabatic warming in this region in both hemispheres throughout the year. These temperature changes can therefore be associated with the intensification of the shallow branch of the BDC (Plumb, 2002; Birner and Bönisch, 2011). The patterns are present in S2 MLO and S5 MLO. Adiabatic cooling in the tropical middle and upper stratosphere, as well as a respective adiabatic warming in the extratropical and polar winter stratosphere indicate the strengthening of the deep branch of the BDC, more pronounced in S5 MLO than in S2 MLO. The strengthening of the BDC would be expected to result in adiabatic cooling directly above the tropopause from increased tropical upwelling. This effect seems to be masked by other processes in Fig. 10. These could be advection or mixing of warm air from the troposphere, or increased longwave (LW) radiation from the warmer troposphere and

potentially more LW absorption in the lowest stratosphere. Lin et al. (2017) found the latter effect to cause strong warming in the tropical tropopause layer. This radiative effect is not accounted for in ~~ΔT_{addst}(SX*-REF*)~~ΔT_{adj}(SX*-REF*), which is the sum of the individual contributions of radiatively active gases to the adjusted stratospheric temperatures. Furthermore, mixing with air out of the upper tropical troposphere could also contribute to the warming patches in the subtropical and extratropical lower stratosphere. This region is particularly affected by mixing (Dietmüller et al., 2018; Eichinger et al., 2019) and mixing itself can also be influenced by climate change (Eichinger et al., 2019).

The deep branch of the residual mean circulation is closely linked to the strength of the winter stratospheric polar vortex. An increase in the poleward flow and in downwelling at higher latitudes is accompanied with a slow down of the stratospheric polar vortex (Kidston et al., 2015, and references therein). The S5 MLO response of zonal mean winds shows indeed an easterly change of the stratospheric polar vortex in boreal winter (DJF) (see Fig. ~~S17~~S15). The respective response for S2 MLO is not significant, but decelerating, too. The SH stratospheric polar vortex strengthens for S2 MLO, but less than in S2 fSST. Nevertheless, the response of stratospheric zonal winds in both MLO experiments is substantially different from fSST in the SH as well.

The easterly change of polar stratospheric zonal winds in the NH during DJF is consistent with the response of the stratospheric polar vortex in CMIP5 global warming simulations (Manzini et al., 2014; Karpechko and Manzini, 2017). Moreover, differences between the fSST and MLO response signals of stratospheric zonal winds during DJF are qualitatively consistent with the results of Karpechko and Manzini (2017). They identified, on the one hand, a deceleration of the stratospheric polar vortex and associated warming in the polar stratosphere in simulations driven by higher SSTs (comparable to the MLO experiments), and, on the other hand, a strengthened and cooled stratospheric polar vortex in simulations driven by CO_2 increase and suppressed tropospheric warming (comparable to the fSST experiments). Karpechko and Manzini (2017) suggested that tropospheric warming and associated strengthening of subtropical winds lead to enhanced wave activity. In S5 MLO subtropical winds strengthen indicating that similar processes might act in our simulations. However, a detailed analysis of wave activity is beyond the scope of this study.

In summary, SST-driven climate feedbacks affect the chemical composition. The differences in stratospheric temperature adjustment between MLO and fSST (see Fig. 9) reflect radiative impacts of these composition changes on stratospheric temperature. Additionally, the patterns of $\Delta\tilde{T}_{\text{dyn.}}$ suggest that dynamical effects have changed significantly in the MLO simulations with respect to fSST. The dynamical temperature response effect for S5 MLO is consistent with the strengthening of the BDC. Dynamic heating counteracts the radiative cooling in the extratropical middle and upper stratosphere and in the subtropical lower stratosphere in S5 MLO. This results in reduced cooling in these regions in S5 MLO in Fig. ~~??~~1 (d), which is not significant on annual average, but in the respective winter hemispheres (not shown). $\Delta\tilde{T}_{\text{dyn.}}$ for S2 MLO indicates strengthening of mainly the shallow branch of the BDC.

~~Figure temperature response in MLO simulations.~~

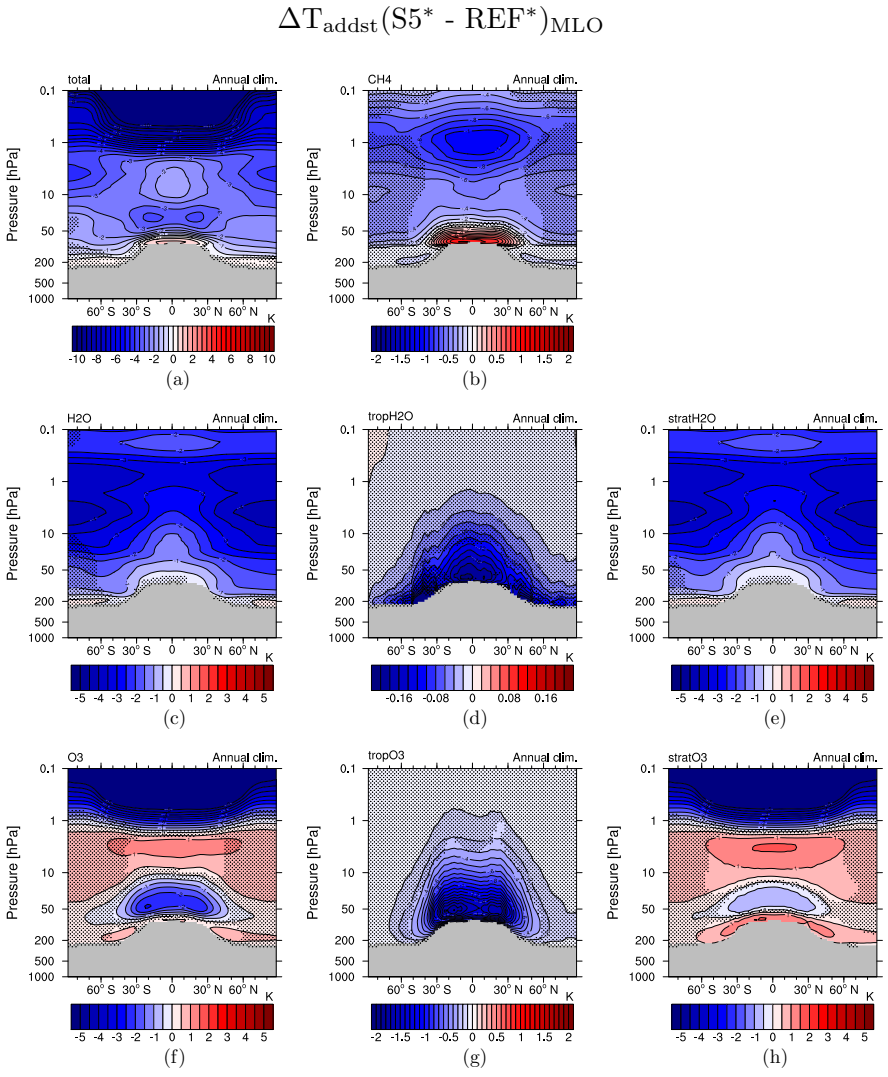

Figure 8. Stratospheric temperature adjustment radiatively induced by individual species changes in simulation S5 MLO ($5\times CH_4$): (a) CH_4, H_2O and O_3 combined, (b) CH_4, (c) H_2O, (d) tropospheric H_2O only, (e) stratospheric H_2O only (SWV), (f) O_3, (g) tropospheric O_3 only and (h) stratospheric O_3 only. Note the different colour bars in panels (a), (b), (d) and (g).

$$\Delta T_{addst}(S5^* - REF^*)_{MLO} - \Delta T_{addst}(S5^* - REF^*)_{fSST}$$

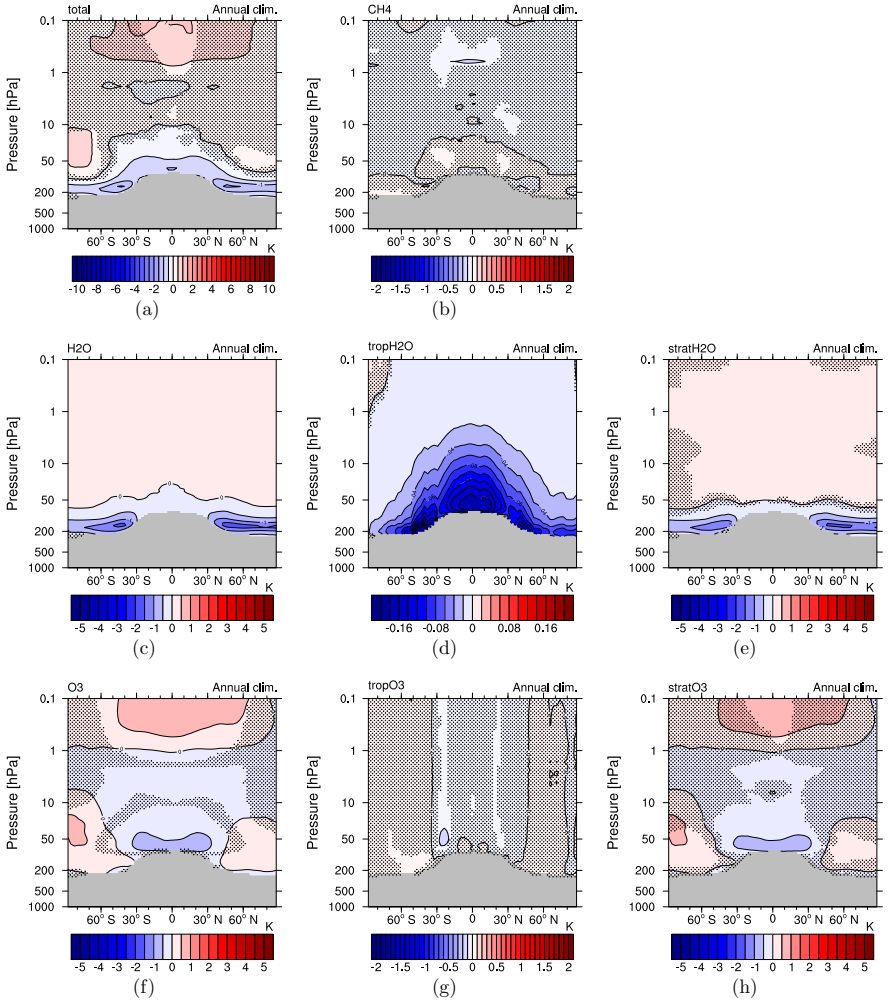

Figure 9. Difference between stratospheric temperature adjustment in simulations S5 MLO and S5 fSST (5×CH_4) radiatively induced by individual species changes: (a) CH_4, H_2O and O_3 combined, (b) CH_4, (c) H_2O, (d) tropospheric H_2O only, (e) stratospheric H_2O only (SWV), (f) O_3, (g) tropospheric O_3 only and (h) stratospheric O_3 only. Note the different colour bars in panels (a), (b), (d) and (g).

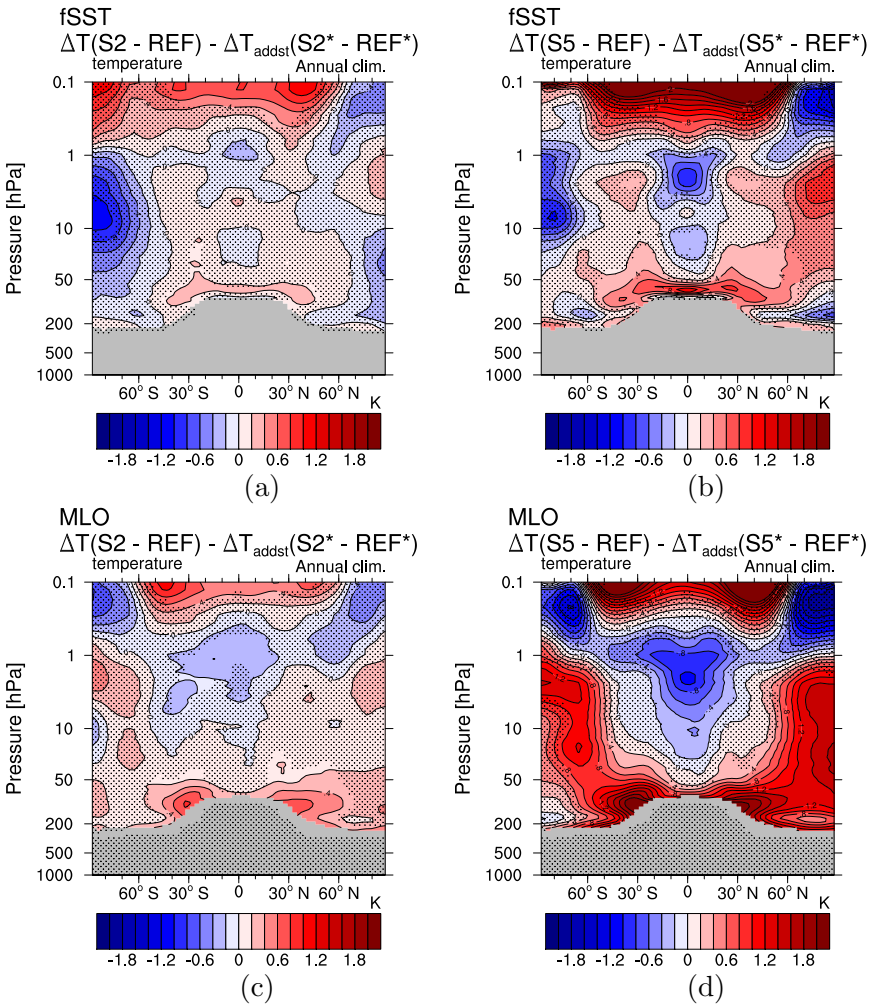

Figure 10. Dynamical temperature response effect of the simulations (a) S2 fSST, (b) S5 fSST, (c) S2 MLO, (d) S5 MLO. The dynamical effect is calculated as the difference between the temperature response in the regular simulations (ΔT(SX-REF) with X either 2 or 5) and the sum of the individual contributions of CH_4, H_2O and O_3 to the adjusted stratospheric temperatures ($\Delta T_{addstadj}$(SX*-REF*) with X either 2 or 5).

4 Summary and Conclusions

While it has been long-since acknowledged that the net RF of CH_4 includes substantial contributions from O_3 and SWV ~~(e.g., IPCC, 2013, Fig. 8.17)~~ (e.g., Fig. 8.17 in IPCC, 2013 derived from Shindell et al., 2009 and Stevenson et al., 2013), it is still common to consider climate feedbacks and climate sensitivity of CH_4 in comparison to CO_2 without accounting for these additional radiative components (Modak et al., 2018; Smith et al., 2018; Richardson et al., 2019). Our study provides a quantification of SST-driven slow radiative feedbacks from CH_4, O_3 and associated SWV changes in climate sensitivity simulations forced by twofold or fivefold CH_4 increase, extending the work of Winterstein et al. (2019) on the respective rapid radiative adjustments.

The strongly enhanced CH_4 mixing ratios cause enhanced depletion of OH in the troposphere. Tropospheric warming, in contrast, results in enhanced OH precursors and causes the reduction of OH in the troposphere to be weaker than in the prescribed SST simulations analysed by Winterstein et al. (2019). Additionally, the acceleration of the CH_4 oxidation at higher temperatures leads to a more efficient depletion of CH_4 in a warming troposphere. This so called climate offset results in a reduced prolongation of the tropospheric CH_4 lifetime and is consistent with previous CCM studies (Voulgarakis et al., 2013). The prolonged tropospheric CH_4 lifetime has the effect that the corresponding CH_4 surface fluxes increase by a smaller factor than the mixing ratio.

Changes in the stratospheric circulation can be clearly identified in the sensitivity simulations that include SST-driven climate feedbacks, on top of the quasi-instantaneous response analysed by Winterstein et al. (2019). Tropospheric warming leads to the acceleration of the BDC in our sensitivity simulations as expected from climate change scenario calculations (Butchart, 2014). In the lower tropical stratosphere, both the decrease of O_3 and the associated cooling, and the increase in CH_4 become more distinct, which reflects the more pronounced acceleration of tropical upwelling induced by a warming troposphere. The strengthening of the BDC also manifests in the temperature response. Whereas the stratospheric polar vortices in both winter hemispheres strengthen in the experiments with prescribed SSTs and SICs, polar stratospheric zonal winds decelerate in northern winter in the sensitivity simulation that include tropospheric warming consistent with the response in CMIP5 global warming simulations (Manzini et al., 2014; Karpechko and Manzini, 2017).

As a result of tropical upper troposphere moistening, increased tropical upwelling and more pronounced warming of the cold point, the transport of tropospheric H_2O into the lower stratosphere is more strongly enhanced in the sensitivity simulations that include SST-driven climate feedbacks, resulting in a stronger increase of SWV in the lower extratropical stratosphere. In the middle and upper stratosphere, where CH_4 oxidation makes an important contribution to SWV, the increase of SWV is weakened in the present sensitivity simulations compared to the quasi-instantaneous response. Less pronounced increases of stratospheric OH in response of the slow adjustments in comparison to the quasi-instantaneous response cause the depletion of CH_4 to be weaker, and thus the in situ source of SWV as well.

The contribution of SST-driven climate feedbacks to the total CH_4 induced O_3 response shows remarkable similarities to the O_3 response to climate feedbacks in CO_2-forced climate change simulations (Dietmüller et al., 2014; Nowack et al., 2018; Chiodo and Polvani, 2019). The consistency between the O_3 feedbacks resulting from these different forcing agents encourages

the separation of the O_3 response patterns into rapid adjustments and climate feedbacks in future studies. Rapid adjustments are specific to the forcing, whereas climate feedbacks are driven by surface temperature changes and are therefore expected to be less dependent on the forcing agent (Sherwood et al., 2015). However, the overall response of O_3 (rapid adjustments and slow feedbacks) is quite different under CH_4 forcing compared to CO_2 forcing owing to chemically induced feedbacks under CH_4 forcing. Chiodo and Polvani (2017); Nowack et al. (2017) suggested that feedbacks from interactive O_3 under CO_2 forcing have the potential to significantly alter the tropospheric circulation. As the overall O_3 response is different under CH_4 forcing, also modified feedbacks on the tropospheric circulation are expected. Those are planned to be assessed using a simulation set-up with a CH_4 emission flux boundary condition to simulate feedbacks of tropospheric CH_4 to changes in its chemical sinks.

The doubled and fivefold CH_4 mixing ratios result in global mean surface temperature changes of 0.42 ± 0.05 K and 1.28 ± 0.04 K, respectively. We estimate the corresponding climate sensitivity parameters λ using these temperature changes and the respective RIs from CH_4 ~~and~~ with the respective chemical adjustments included, as determined by Winterstein et al. (2019), that can well be interpreted as the corresponding ERFs. The respective estimate of λ for $5\times CH_4$ compares well with an estimate from CO_2-driven climate change simulations with EMAC with comparable magnitude of RI (Rieger et al., 2017), suggesting an efficacy of CH_4 ERF close to one. The estimate of λ corresponding to $2\times CH_4$ is smaller than the respective value for $5\times CH_4$, but has a large uncertainty. Considering the large uncertainty and intermodel spread (Richardson et al., 2019) of this parameter, we conclude that a more targeted experimental design is necessary to exactly quantify the effect of chemical feedbacks on the climate sensitivity in CH_4-driven scenarios and its efficacy with respect to CO_2 forcing.

The RIs from the purely SST-driven response of CH_4 and O_3 are small. The RIs resulting from changes of tropospheric and stratospheric H_2O are enlarged by SST-driven climate feedbacks. Increased tropospheric humidity in a warming troposphere enhances the RI. The reason for the enlarged RI from SWV is its more pronounced increase in the lower stratosphere, where its changes dominate the induced RI (Solomon et al., 2010). As the increase of SWV in this region is likely induced by transport from the warmer tropical troposphere, this part of the RI increase cannot be regarded to be ~~a chemically induced rapid adjustment~~chemically induced. The associated responses of stratospheric adjusted temperatures from the purely SST-driven response are dominated by the just explained changes of SWV and by decreases of stratospheric O_3 in the lowermost tropical stratosphere. It is worth noting, that tropospheric CH_4 mixing ratios do not respond to changes in tropospheric sinks (e.g. OH) in the used simulation set-up, as its mixing ratio is prescribed at the lower boundary. The prolongation of the tropospheric CH_4 lifetime indicates a positive feedback on the CH_4 mixing ratio, and thus on the induced RI. In a future study, climate change scenario simulations conducted with a CCM with realistic CH_4 emission fluxes are planned to quantify this chemical feedback of CH_4.

In the present study we are able for the first time to quantify the effects of slow climate feedbacks on the chemical composition and circulation in CH_4-forced climate change scenarios and further evaluate them in comparison to the quasi-instantaneous atmospheric response.

Code and data availability. The Modular Earth Submodel System (MESSy) is continuously developed and applied by a consortium of institutions. The usage of MESSy and access to the source code is licensed to all affiliates of institutions, which are members of the MESSy Consortium. Institutions can become members of the MESSy Consortium by signing the MESSy Memorandum of Understanding. More information can be found on the MESSy Consortium website (https://www.messy-interface.org/, last access: 27 May 2020, Jöckel P. and the MESSy Consortium). Furthermore the exact code version used to produce the simulation results is archived at the German Climate Computing Center (DKRZ) and can be made available to members of the MESSy community upon request. The simulation results are also archived at DKRZ and are available opon request.

Appendix A

The MLO simulations were carried out with a more recent MESSy version with regard to the fSST simulations (2.54.0 instead of 2.52). This involves changes to the chemistry module MECCA (Sander et al., 2011) including the update of reaction rate coefficients to the latest recommendations, Evaluation No. 18, of the Jet Propulsion Laboratory (Burkholder et al., 2015) and to values coming from other recent laboratory studies. A table of all affected reactions can be found in the Supplement (Tab. S1). Moreover, the yield of the photolysis of $CFCl_3$ (CFC-11) and CF_2Cl_2 (CFC-12) changed from three and two, respectively, to one chlorine (Cl) atom. The smaller Cl yield influences the O_3 mixing ratio in the stratosphere as Cl acts as a catalyst in the O_3 depleting cycles. The O_3 mixing ratio is higher everywhere in the stratosphere, except in the lowermost tropical stratosphere, in REF MLO compared to REF fSST (see Fig. ~~S19~~S17). This results further in higher temperatures in the stratosphere in REF MLO (not shown). The contribution of the ClO_x O_3 depleting cycle on total O_3 loss peaks at around 40 to 45 km altitude (see Fig. 5.28 in Seinfeld and Pandis, 2016). This corresponds approximately to the altitude of the maximum relative difference of O_3 mixing ratio between REF MLO and REF fSST (see Fig. ~~S19~~S17).

Appendix B

In the REF QFLX simulation the setting of the non-orographic gravity wave drag parameterization (GWAVE, Baumgaertner et al., 2013) was different than in all the other simulations (fSST and MLO), in which breaking of gravity waves transfers only momentum, but no heat. In REF QFLX heat is also transferred leading to higher temperatures in the mesosphere. Since predominantly the mesosphere is affected, the different setting does not considerably influence the retrieved heat flux correction at the surface, the determination of which is the purpose of REF QFLX.

Author contributions. The simulations were set-up and carried out by PJ and FW with contributions of MK in applying the MLOCEAN submodel. MP and FW contrived and carried out the radiative impact and stratospheric adjusted temperature calculations and FW created the corresponding figures. LS analysed the data, created the remaining figures and prepared the manuscript with significant contributions regarding the interpretation and evaluation of the model results from all coauthors.

Competing interests. The authors declare that they have no conflict of interest.

Acknowledgements. We acknowledge the financial support by the DFG Project WI 5369/1-1 and the DLR internal projects KliSAW (Klimarelevanz von atmosphärischen Spurengasen, Aerosolen und Wolken) and MABAK (Innovative Methoden zur Analyse und Bewertung von Veränderungen der Atmosphäre und des Klimasystems). The model simulations have been performed at the German Climate Computing Centre (DKRZ) through support from the Bundesministerium für Bildung und Forschung (BMBF). We used the Climate Data Operators (CDO; https://code.mpimet.mpg.de/projects/cdo) for data processing and the NCAR Command Language (NCL; https://doi.org/10.5065/D6WD3XH5) for data analysis and to create the figures of this study. We furthermore thank all contributors of the project ESCiMo (Earth System Chemistry integrated Modelling), which provides the model configuration and initial conditions. We thank Roland Eichinger for his constructive internal review of the manuscript and Hella Garny for her helpful comments on the interpretation of the dynamically induced temperature response. Finally, we thank Holger Tost for editing this manuscript, and Peer Johannes Nowack and one anonymous reviewer for their comments that improved the manuscript.

References

Austin, J., Wilson, J., Li, F., and Vömel, H.: Evolution of Water Vapor Concentrations and Stratospheric Age of Air in Coupled Chemistry–Climate Model Simulations, J. Atmos. Sci., 64, 905–921, https://doi.org/10.1175/JAS3866.1, 2007.

Baumgaertner, A. J. G., Jöckel, P., Aylward, A. D., and Harris, M. J.: Climate and Weather of the Sun-Earth System (CAWSES), chap. Simulation of Particle Precipitation Effects on the Atmosphere with the MESSy Model System, pp. 301–316, Springer Atmospheric Sciences, Springer Netherlands, https://doi.org/10.1007/978-94-007-4348-9_17, 2013.

Birner, T. and Bönisch, H.: Residual circulation trajectories and transit times into the extratropical lowermost stratosphere, Atmos. Chem. Phys., 11, 817–827, https://doi.org/10.5194/acp-11-817-2011, https://www.atmos-chem-phys.net/11/817/2011/, 2011.

Bony, S., Bellon, G., Klocke, D., Sherwood, S., Fermepin, S., and Denvil, S.: Robust direct effect of carbon dioxide on tropical circulation and regional precipitation, Nature Geoscience, 6, 447–451, https://doi.org/10.1038/ngeo1799, 2013.

Burkholder, J. B., Sander, S. P., Abbatt, J. P. D., Barker, J. R., Huie, R. E., Kolb, C. E., Kurylo, M. J., Orkin, V. L., Wilmouth, D. M., and Wine, P. H.: Chemical Kinetics and Photochemical Data for Use in Atmospheric Studies, Evaluation No. 18, JPL Publication 15-10, Jet Propulsion Laboratory, http://jpldataeval.jpl.nasa.gov/, 2015.

Butchart, N.: The Brewer-Dobson circulation, Rev. Geophys., 52, 157–184, https://doi.org/10.1002/2013RG000448, 2014.

Butchart, N. and Scaife, A. A.: Removal of chlorofluorocarbons by increased mass exchange between the stratosphere and troposphere in a changing climate, Nature, 410, 799–802, https://doi.org/10.1038/35071047, https://doi.org/10.1038/35071047, 2001.

Chiodo, G. and Polvani, L. M.: Reduced Southern Hemispheric circulation response to quadrupled CO_2 due to stratospheric ozone feedback, Geophys. Res. Lett., 44, 465–474, https://doi.org/10.1002/2016GL071011, 2017.

Chiodo, G. and Polvani, L. M.: The Response of the Ozone Layer to Quadrupled CO_2 Concentrations: Implications for Climate, J. Climate, 32, 7629–7642, https://doi.org/10.1175/JCLI-D-19-0086.1, https://doi.org/10.1175/JCLI-D-19-0086.1, 2019.

Colman, R. A. and McAvaney, B. J.: On tropospheric adjustment to forcing and climate feedbacks, Clim. Dyn., 36, 1649–1658, https://doi.org/10.1007/s00382-011-1067-4, https://doi.org/10.1007/s00382-011-1067-4, 2011.

Danabasoglu, G. and Gent, P. R.: Equilibrium climate sensitivity: Is it accurate to use a slab ocean model?, J. Climate, 22, 2494–2499, https://doi.org/10.1175/2008JCLI2596.1, 2009.

Dean, J. F., Middelburg, J. J., Röckmann, T., Aerts, R., Blauw, L. G., Egger, M., Jetten, M. S. M., de Jong, A. E. E., Meisel, O. H., Rasigraf, O., Slomp, C. P., in't Zandt, M. H., and Dolman, A. J.: Methane Feedbacks to the Global Climate System in a Warmer World, Rev. Geophys., 56, 207–250, https://doi.org/10.1002/2017RG000559, https://agupubs.onlinelibrary.wiley.com/doi/abs/10.1002/2017RG000559, 2018.

Dietmüller, S., Ponater, M., and Sausen, R.: Interactive ozone induces a negative feedback in CO_2-driven climate change simulations, J. Geophys. Res. Atmos., 119, 1796–1805, https://doi.org/10.1002/2013JD020575, https://agupubs.onlinelibrary.wiley.com/doi/full/10.1002/2013JD020575, 2014.

Dietmüller, S., Jöckel, P., Tost, H., Kunze, M., Gellhorn, C., Brinkop, S., Frömming, C., Ponater, M., Steil, B., Lauer, A., and Hendricks, J.: A new radiation infrastructure for the Modular Earth Submodel System (MESSy, based on version 2.51), Geosci. Model Dev., 9, 2209–2222, https://doi.org/10.5194/gmd-9-2209-2016, https://www.geosci-model-dev.net/9/2209/2016/, 2016.

Dietmüller, S., Eichinger, R., Garny, H., Birner, T., Boenisch, H., Pitari, G., Mancini, E., Visioni, D., Stenke, A., Revell, L., Rozanov, E., Plummer, D. A., Scinocca, J., Jöckel, P., Oman, L., Deushi, M., Kiyotaka, S., Kinnison, D. E., Garcia, R., Morgenstern, O., Zeng, G., Stone, K. A., and Schofield, R.: Quantifying the effect of mixing on the mean age of air in CCMVal-2 and CCMI-1 models, Atmos. Chem. Phys., 18, 6699–6720, https://doi.org/10.5194/acp-18-6699-2018, https://www.atmos-chem-phys.net/18/6699/2018/, 2018.

Dunne, J. P., Winton, M., Bacmeister, J., Danabasoglu, G., Gettelman, A., Golaz, J.-C., Hannay, C., Schmidt, G. A., Krasting, J. P., Leung, L. R., Nazarenko, L., Sentman, L. T., Stouffer, R. J., and Wolfe, J. D.: Comparison of Equilibrium Climate Sensitivity Estimates From Slab Ocean, 150-Year, and Longer Simulations, Geophys. Res. Lett., 47, e2020GL088 852, https://doi.org/10.1029/2020GL088852, https://agupubs.onlinelibrary.wiley.com/doi/abs/10.1029/2020GL088852, 2020.

Eichinger, R., Dietmüller, S., Garny, H., Šácha, P., Birner, T., Bönisch, H., Pitari, G., Visioni, D., Stenke, A., Rozanov, E., Revell, L., Plummer, D. A., Jöckel, P., Oman, L., Deushi, M., Kinnison, D. E., Garcia, R., Morgenstern, O., Zeng, G., Stone, K. A., and Schofield, R.: The influence of mixing on the stratospheric age of air changes in the 21st century, Atmospheric Chemistry and Physics, 19, 921–940, https://doi.org/10.5194/acp-19-921-2019, https://www.atmos-chem-phys.net/19/921/2019/, 2019.

Forster, P. M., Richardson, T., Maycock, A. C., Smith, C. J., Samset, B. H., Myhre, G., Andrews, T., Pincus, R., and Schulz, M.: Recommendations for diagnosing effective radiative forcing from climate models for CMIP6, J. Geophys. Res. Atmos., 121, 12 460–12 475, https://doi.org/10.1002/2016JD025320, https://agupubs.onlinelibrary.wiley.com/doi/abs/10.1002/2016JD025320, 2016.

Frank, F., Jöckel, P., Gromov, S., and Dameris, M.: Investigating the yield of H_2O and H_2 from methane oxidation in the stratosphere, Atmos. Chem. Phys., 18, 9955–9973, https://doi.org/10.5194/acp-18-9955-2018, https://www.atmos-chem-phys.net/18/9955/2018/, 2018.

Garcia, R. R. and Randel, W. J.: Acceleration of the Brewer–Dobson Circulation due to Increases in Greenhouse Gases, J. Atmos. Sci., 65, 2731–2739, https://doi.org/10.1175/2008JAS2712.1, https://doi.org/10.1175/2008JAS2712.1, 2008.

Geoffroy, O., Saint-Martin, D., Voldoire, A., Salas y Melia, D., and Senesi, S.: Adjusted radiative forcing and global radiative feedbacks in CNRM-CM5, a closure of the partial decomposition, Clim. Dyn., 42, 1807–1818, https://doi.org/10.1007/s00382-013-1741-9, 2014.

Gregory, J. M., Ingram, W. J., Palmer, M. A., Jones, G. S., Stott, P. A., Thorpe, R. B., Lowe, J. A., Johns, T. C., and Williams, K. D.: A new method for diagnosing radiative forcing and climate sensitivity, Geophys. Res. Lett., 31, https://doi.org/10.1029/2003GL018747, https://agupubs.onlinelibrary.wiley.com/doi/abs/10.1029/2003GL018747, 2004.

Hansen, J., Sato, M., Ruedy, R., Nazarenko, L., Lacis, A., Schmidt, G. A., Russell, G., Aleinov, I., Bauer, M., Bauer, S., Bell, N., Cairns, B., Canuto, V., Chandler, M., Cheng, Y., Del Genio, A., Faluvegi, G., Fleming, E., Friend, A., Hall, T., Jackman, C., Kelley, M., Kiang, N., Koch, D., Lean, J., Lerner, J., Lo, K., Menon, S., Miller, R., Minnis, P., Novakov, T., Oinas, V., Perlwitz, J., Perlwitz, J., Rind, D., Romanou, A., Shindell, D., Stone, P., Sun, S., Tausnev, N., Thresher, D., Wielicki, B., Wong, T., Yao, M., and Zhang, S.: Efficacy of climate forcings, J. Geophys. Res. Atmos, 110, https://doi.org/10.1029/2005JD005776, https://agupubs.onlinelibrary.wiley.com/doi/abs/10.1029/2005JD005776, 2005.

Hein, R., Dameris, M., Schnadt, C., Land, C., Grewe, V., Köhler, I., Ponater, M., Sausen, R., Steil, B., Landgraf, J., and Brühl, C.: Results of an interactively coupled atmospheric chemistry - general circulation model: Comparison with observations, Ann. Geophys., 19, 435–457, https://doi.org/10.5194/angeo-19-435-2001, 2001.

IPCC: Climate Change 2013: The Physical Science Basis. Contribution of Working Group I to the Fifth Assessment Report of the Intergovernmental Panel on Climate Change [Stocker, T.F., D. Qin, G.-K. Plattner, M. Tignor, S.K. Allen, J. Boschung, A. Nauels, Y. Xia, V. Bex and P.M. Midgley (eds.)], Cambridge University Press, Cambridge, United Kingdom and New York, NY, USA, https://doi.org/10.1017/CBO9781107415324, www.climatechange2013.org, 2013.

Jöckel, P., Tost, H., Pozzer, A., Brühl, C., Buchholz, J., Ganzeveld, L., Hoor, P., Kerkweg, A., Lawrence, M. G., Sander, R., Steil, B., Stiller, G., Tanarhte, M., Taraborrelli, D., van Aardenne, J., and Lelieveld, J.: The atmospheric chemistry general circulation model ECHAM5/MESSy1: consistent simulation of ozone from the surface to the mesosphere, Atmos. Chem. Phys., 6, 5067–5104, https://doi.org/10.5194/acp-6-5067-2006, 2006.

Jöckel, P., Tost, H., Pozzer, A., Kunze, M., Kirner, O., Brenninkmeijer, C. A. M., Brinkop, S., Cai, D. S., Dyroff, C., Eckstein, J., Frank, F., Garny, H., Gottschaldt, K.-D., Graf, P., Grewe, V., , Kerkweg, A., Kern, B., Matthes, S., Mertens, M., Meul, S., Neumaier, M., Nützel, M., Oberländer-Hayn, S., Ruhnke, R., Runde, T., Sander, R., Scharffe, D., and Zahn, A.: Earth System Chemistry integrated Modelling (ESCiMo) with the Modular Earth Submodel System (MESSy) version 2.51, Geosci. Model Dev., 9, 1153–1200, https://doi.org/10.5194/gmd-9-1153-2016, http://www.geosci-model-dev.net/9/1153/2016/gmd-9-1153-2016.html, 2016.

Jöckel P. and the MESSy Consortium: The highly structured Modular Earth Submodel System (MESSy), http://www.messy-interface.org, last access: 27 May 2020.

Karpechko, A. Y. and Manzini, E.: Arctic Stratosphere Dynamical Response to Global Warming, J. Climate, 30, 7071–7086, https://doi.org/10.1175/JCLI-D-16-0781.1, https://doi.org/10.1175/JCLI-D-16-0781.1, 2017.

Kerkweg, A., Sander, R., Tost, H., and Jöckel, P.: Technical note: Implementation of prescribed (OFFLEM), calculated (ONLEM), and pseudo-emissions (TNUDGE) of chemical species in the Modular Earth Submodel System (MESSy), Atmos. Chem. Phys., 6, 3603–3609, https://doi.org/10.5194/acp-6-3603-2006, https://www.atmos-chem-phys.net/6/3603/2006/, 2006.

Kidston, J., Scaife, A. A., Hardiman, S. C., Mitchell, D. M., Butchart, N., Baldwin, M. P., and Gray, L. J.: Stratospheric influence on tropospheric jet streams, storm tracks and surface weather, Nature Geoscience, 8, 433–440, https://doi.org/10.1038/ngeo2424, https://doi.org/10.1038/ngeo2424, 2015.

Kirner, O., Ruhnke, R., and Sinnhuber, B.-M.: Chemistry–Climate Interactions of Stratospheric and Mesospheric Ozone in EMAC Long-Term Simulations with Different Boundary Conditions for CO_2, CH_4, N_2O, and ODS, Atmosphere-Ocean, 53, 140–152, https://doi.org/10.1080/07055900.2014.980718, 2015.

Klappenbach, F., Bertleff, M., Kostinek, J., Hase, F., Blumenstock, T., Agusti-Panareda, A., Razinger, M., and Butz, A.: Accurate mobile remote sensing of XCO_2 and XCH_4 latitudinal transects from aboard a research vessel, Atmos. Meas. Tech., 8, 5023–5038, https://doi.org/10.5194/amt-8-5023-2015, https://www.atmos-meas-tech.net/8/5023/2015/, 2015.

Kunze, M., Godolt, M., Langematz, U., Grenfell, J., Hamann-Reinus, A., and Rauer, H.: Investigating the early Earth faint young Sun problem with a general circulation model, Planet. Space Sci., 98, 77–92, https://doi.org/10.1016/j.pss.2013.09.011, http://www.sciencedirect.com/science/article/pii/S0032063313002389, planetary evolution and life, 2014.

Lawrence, M. G., Jöckel, and von Kuhlmann, R.: What does the global mean OH concentration tell us?, Atmos. Chem. Phys., 1, 37–49, www.atmos-chem-phys.org/acp/1/37/, 2001.

Li, C., von Storch, J.-S., and Marotzke, J.: Deep-ocean heat uptake and equilibrium climate response, Clim. Dyn., 40, 1071–1086, https://doi.org/10.1007/s00382-012-1350-z, 2013.

Lin, P., Paynter, D., Ming, Y., and Ramaswamy, V.: Changes of the Tropical Tropopause Layer under Global Warming, J. Climate, 30, 1245–1258, https://doi.org/10.1175/JCLI-D-16-0457.1, https://doi.org/10.1175/JCLI-D-16-0457.1, 2017.

Manzini, E., Karpechko, A. Y., Anstey, J., Baldwin, M. P., Black, R. X., Cagnazzo, C., Calvo, N., Charlton-Perez, A., Christiansen, B., Davini, P., Gerber, E., Giorgetta, M., Gray, L., Hardiman, S. C., Lee, Y.-Y., Marsh, D. R., McDaniel, B. A., Purich, A., Scaife, A. A., Shindell, D., Son, S.-W., Watanabe, S., and Zappa, G.: Northern winter climate change: Assessment of uncertainty in CMIP5 projections related to stratosphere-troposphere coupling, J. Geophys. Res. Atmos., 119, 7979–7998, https://doi.org/10.1002/2013JD021403, https://agupubs.onlinelibrary.wiley.com/doi/abs/10.1002/2013JD021403, 2014.

Modak, A., Bala, G., Caldeira, K., and Cao, L.: Does shortwave absorption by methane influence its effectiveness?, Climate Dyn., 51, 3653–3672, https://doi.org/10.1007/s00382-018-4102-x, 2018.

Morgenstern, O., Stone, K. A., Schofield, R., Akiyoshi, H., Yamashita, Y., Kinnison, D. E., Garcia, R. R., Sudo, K., Plummer, D. A., Scinocca, J., Oman, L. D., Manyin, M. E., Zeng, G., Rozanov, E., Stenke, A., Revell, L. E., Pitari, G., Mancini, E., Di Genova, G., Visioni, D., Dhomse, S. S., and Chipperfield, M. P.: Ozone sensitivity to varying greenhouse gases and ozone-depleting substances in CCMI-1 simulations, Atmos. Chem. Phys., 18, 1091–1114, https://doi.org/10.5194/acp-18-1091-2018, https://www.atmos-chem-phys.net/18/1091/2018/, 2018.

Nisbet, E. G., Manning, M. R., Dlugokencky, E. J., Fisher, R. E., Lowry, D., Michel, S. E., Myhre, C. L., Platt, S. M., Allen, G., Bousquet, P., Brownlow, R., Cain, M., France, J. L., Hermansen, O., Hossaini, R., Jones, A. E., Levin, I., Manning, A. C., Myhre, G., Pyle, J. A., Vaughn, B. H., Warwick, N. J., and White, J. W. C.: Very Strong Atmospheric Methane Growth in the 4 Years 2014–2017: Implications for the Paris Agreement, Glob. Biogeochem. Cycles, 33, 318–342, https://doi.org/10.1029/2018GB006009, https://agupubs.onlinelibrary.wiley.com/doi/abs/10.1029/2018GB006009, 2019.

Nowack, P. J., Braesicke, P., Luke Abraham, N., and Pyle, J. A.: On the role of ozone feedback in the ENSO amplitude response under global warming, Geophys. Res. Lett., 44, 3858–3866, https://doi.org/10.1002/2016GL072418, https://agupubs.onlinelibrary.wiley.com/doi/abs/10.1002/2016GL072418, 2017.

Nowack, P. J., Abraham, N. L., Braesicke, P., and Pyle, J. A.: The Impact of Stratospheric Ozone Feedbacks on Climate Sensitivity Estimates, J. Geophys. Res. Atmos., 123, 4630–4641, https://doi.org/10.1002/2017JD027943, https://agupubs.onlinelibrary.wiley.com/doi/abs/10.1002/2017JD027943, 2018.

Plumb, R. A.: Stratospheric Transport, Journal of the Meteorological Society of Japan. Ser. II, 80, 793–809, https://doi.org/10.2151/jmsj.80.793, 2002.

Randel, W. and Park, M.: Diagnosing Observed Stratospheric Water Vapor Relationships to the Cold Point Tropical Tropopause, J. Geophys. Res. Atmos., 124, 7018–7033, https://doi.org/10.1029/2019JD030648, https://agupubs.onlinelibrary.wiley.com/doi/full/10.1029/2019JD030648, 2019.

Rayner, N. A., Parker, D. E., Horton, E. B., Folland, C. K., Alexander, L. V., Rowell, D. P., Kent, E. C., and Kaplan, A.: Global analyses of sea surface temperature, sea ice, and night marine air temperature since the late nineteenth century, J. Geophys. Res. Atmos., 108, https://doi.org/10.1029/2002JD002670, 4407, 2003.

Revell, L., Stenke, A., Rozanov, E., Ball, W., Lossow, S., and Peter, T.: The role of methane in projections of 21st century stratospheric water vapour, Atmos. Chem. Phys., 16, 13 067–13 080, https://doi.org/10.5194/acp-16-13067-2016, www.atmos-chem-phys.net/16/13067/2016/, 2016.

Richardson, T. B., Forster, P. M., Smith, C. J., Maycock, A. C., Wood, T., Andrews, T., Boucher, O., Faluvegi, G., Fläschner, D., Hodnebrog, Ø., Kasoar, M., Kirkevåg, A., Lamarque, J.-F., Mülmenstädt, J., Myhre, G., Olivié, D., Portmann, R. W., Samset, B. H., Shawki, D., Shindell, D., Stier, P., Takemura, T., Voulgarakis, A., and Watson-Parris, D.: Efficacy of Climate Forcings in PDRMIP Models, J. Geophys. Res. Atmos., 124, 12 824–12 844, https://doi.org/10.1029/2019JD030581, https://agupubs.onlinelibrary.wiley.com/doi/abs/10.1029/2019JD030581, 2019.

Rieger, V. S., Dietmüller, S., and Ponater, M.: Can feedback analysis be used to uncover the physical origin of climate sensitivity and efficacy differences?, Climate Dyn., 49, 2831–2844, https://doi.org/10.1007/s00382-016-3476-x, https://link.springer.com/article/10.1007%2Fs00382-016-3476-x, 2017.

Rind, D., Suozzo, R., Balachandran, N. K., and Prather, M. J.: Climate Change and the Middle Atmosphere Part I: The Doubled CO_2 Climate, American Meterological Society, 47, 475–494, 1990.

Röckmann, T., Brass, M., Borchers, R., and Engel, A.: The isotopic composition of methane in the stratosphere: high-altitude balloon sample measurements, Atmos. Chem. Phys., 11, 13 287–13 304, https://doi.org/10.5194/acp-11-13287-2011, 2011.

Roeckner, E., Siebert, T., and Feichter, J.: Climatic response to anthropogenic sulfate forcing simulated with a general circulation model, Aerosol Forcing of Climate, pp. 349–362, 1995.

Rohs, S., Schiller, C., Riese, M., Engel, A., Schmidt, U., Wetter, T., Levin, I., Nakazawa, T., and Aoki, S.: Long-term changes of methane and hydrogen in the stratosphere in the period 1978-2003 and their impact on the abundance of stratospheric water vapor, J. Geophys. Res. Atmos., 111, 1–12, https://doi.org/10.1029/2005JD006877, 2006.

Rosier, S. M. and Shine, K. P.: The effect of two decades of ozone change on stratospheric temperature as indicated by a general circulation model, Geophys. Res. Lett., 27, 2617–2620, https://doi.org/10.1029/2000GL011584, https://agupubs.onlinelibrary.wiley.com/doi/abs/10.1029/2000GL011584, 2000.

Sander, R., Baumgaertner, A., Gromov, S., Harder, H., Jöckel, P., Kerkweg, A., Kubistin, D., Regelin, E., Riede, H., Sandu, A., Taraborrelli, D., Tost, H., and Xie, Z.-Q.: The atmospheric chemistry box model CAABA/MECCA-3.0, Geosci. Model Dev., 4, 373–380, https://doi.org/10.5194/gmd-4-373-2011, 2011.

Saunois, M., Bousquet, P., Poulter, B., Peregon, A., Ciais, P., Canadell, J. G., Dlugokencky, E. J., Etiope, G., Bastviken, D., Houweling, S., Janssens-Maenhout, G., Tubiello, F. N., Castaldi, S., Jackson, R. B., Alexe, M., Arora, V. K., Beerling, D. J., Bergamaschi, P., Blake, D. R., Brailsford, G., Brovkin, V., Bruhwiler, L., Crevoisier, C., Crill, P., Covey, K., Curry, C., Frankenberg, C., Gedney, N., Höglund-Isaksson, L., Ishizawa, M., Ito, A., Joos, F., Kim, H.-S., Kleinen, T., Krummel, P., Lamarque, J.-F., Langenfelds, R., Locatelli, R., Machida, T., Maksyutov, S., McDonald, K. C., Marshall, J., Melton, J. R., Morino, I., Naik, V., O'Doherty, S., Parmentier, F.-J. W., Patra, P. K., Peng, C., Peng, S., Peters, G. P., Pison, I., Prigent, C., Prinn, R., Ramonet, M., Riley, W. J., Saito, M., Santini, M., Schroeder, R., Simpson, I. J., Spahni, R., Steele, P., Takizawa, A., Thornton, B. F., Tian, H., Tohjima, Y., Viovy, N., Voulgarakis, A., van Weele, M., van der Werf, G. R., Weiss, R., Wiedinmyer, C., Wilton, D. J., Wiltshire, A., Worthy, D., Wunch, D., Xu, X., Yoshida, Y., Zhang, B., Zhang, Z., and Zhu, Q.: The global methane budget 2000–2012, Earth Syst. Sci. Data, 8, 697–751, https://doi.org/10.5194/essd-8-697-2016, https://www.earth-syst-sci-data.net/8/697/2016/, 2016a.

Saunois, M., Jackson, R. B., Bousquet, P., Poulter, B., and Canadell, J. G.: The growing role of methane in anthropogenic climate change, Environ. Res. Lett., 11, 120 207, https://doi.org/10.1088/1748-9326/11/12/120207, http://stacks.iop.org/1748-9326/11/i=12/a=120207, 2016b.

Schnadt, C., Dameris, M., Ponater, M., Hein, R., Grewe, V., and Steil, B.: Interaction of atmospheric chemistry and climate and its impact on stratospheric ozone, Climate Dyn., 18, 501–517, https://doi.org/10.1007/s00382-001-0190-z, https://link.springer.com/article/10.1007/s00382-001-0190-z, 2002.

Seinfeld, J. H. and Pandis, S. N.: Atmospheric Chemistry and Physics: From Air Pollution to Climate Change, John Wiley & Sons, Inc., third edn., 2016.

Sherwood, S. C., Bony, S., Boucher, O., Bretherton, C., Forster, P. M., Gregory, J. M., and Stevens, B.: Adjustments in the Forcing-Feedback Framework for Understanding Climate Change, Bulletin of the American Meteorological Society, 96, 217–228, https://doi.org/10.1175/BAMS-D-13-00167.1, https://doi.org/10.1175/BAMS-D-13-00167.1, 2015.

Shindell, D. T., Faluvegi, G., Bell, N., and Schmidt, G. A.: An emissions-based view of climate forcing by methane and tropospheric ozone, Geophys. Res. Lett., 32, 1–4, https://doi.org/10.1029/2004GL021900, 2005.

Shindell, D. T., Faluvegi, G., Koch, D. M., Schmidt, G. A., Unger, N., and Bauer, S. E.: Improved Attribution of Climate Forcing to Emissions, Science, 326, 716–718, https://doi.org/10.1126/science.1174760, https://science.sciencemag.org/content/326/5953/716, 2009.

Shine, K. P., Cook, J., Highwood, E. J., and Joshi, M. M.: An alternative to radiative forcing for estimating the relative importance of climate change mechanisms, Geophys. Res. Lett., 30, https://doi.org/10.1029/2003GL018141, https://agupubs.onlinelibrary.wiley.com/doi/abs/10.1029/2003GL018141, 2003.

Smith, C. J., Kramer, R. J., Myhre, G., Forster, P. M., Soden, B., Andrews, T., Boucher, O., Faluvegi, G., Fläschner, D., Hodnebrog, Ø. ., Kasoar, M., Kharin, V., Kirkevåg, A., Lamarque, J.-F., Mülmenstädt, J., Olivié, D., Richardson, T., Samset, B. H., Shindell, D., Stier, P., Takemura, T., Voulgarakis, A., and Watson-Parris, D.: Understanding Rapid Adjustments to Diverse Forcing Agents, Geophys. Res. Lett., 45, 12,023–12,031, https://doi.org/10.1029/2018GL079826, https://agupubs.onlinelibrary.wiley.com/doi/abs/10.1029/2018GL079826, 2018.

Smith, C. J., Kramer, R. J., Myhre, G., Alterskjær, K., Collins, W., Sima, A., Boucher, O., Dufresne, J.-L., Nabat, P., Michou, M., Yukimoto, S., Cole, J., Paynter, D., Shiogama, H., O'Connor, F. M., Robertson, E., Wiltshire, A., Andrews, T., Hannay, C., Miller, R., Nazarenko, L., Kirkevåg, A., Olivié, D., Fiedler, S., Lewinschal, A., Mackallah, C., Dix, M., Pincus, R., and Forster, P. M.: Effective radiative forcing and adjustments in CMIP6 models, Atmospheric Chemistry and Physics, 20, 9591–9618, https://doi.org/10.5194/acp-20-9591-2020, https://acp.copernicus.org/articles/20/9591/2020/, 2020.

Solomon, S., Rosenlof, K. H., Portmann, R. W., Daniel, J. S., Davis, S. M., Sanford, T. J., and Plattner, G.-K.: Contributions of Stratospheric Water Vapor to Decadal Changes in the Rate of Global Warming, Science, 327, 1219–1223, https://doi.org/10.1126/science.1182488, 2010.

Stevenson, D. S., Young, P. J., Naik, V., Lamarque, J.-F., Shindell, D. T., Voulgarakis, A., Skeie, R. B., Dalsoren, S. B., Myhre, G., Berntsen, T. K., Folberth, G. A., Rumbold, S. T., Collins, W. J., MacKenzie, I. A., Doherty, R. M., Zeng, G., van Noije, T. P. C., Strunk, A., Bergmann, D., Cameron-Smith, P., Plummer, D. A., Strode, S. A., Horowitz, L., Lee, Y. H., Szopa, S., Sudo, K., Nagashima, T., Josse, B., Cionni, I., Righi, M., Eyring, V., Conley, A., Bowman, K. W., Wild, O., and Archibald, A.: Tropospheric ozone changes, radiative forcing and attribution to emissions in the Atmospheric Chemistry and Climate Model Intercomparison Project (ACCMIP), Atmos. Chem. and Phys., 13, 3063–3085, https://doi.org/10.5194/acp-13-3063-2013, https://acp.copernicus.org/articles/13/3063/2013/, 2013.

Stuber, N., Sausen, R., and Ponater, M.: Stratosphere adjusted radiative forcing calculations in a comprehensive climate model, Theor. Appl. Climatol., 68, 125–135, https://doi.org/10.1007/s007040170041, 2001.

Voulgarakis, A., Naik, V., Lamarque, J.-F., Shindell, D. T., Young, P. J., Prather, M. J., Wild, O., Field, R. D., Bergmann, D., Cameron-Smith, P., Cionni, I., Collins, W. J., Dalsøren, S. B., Doherty, R. M., Eyring, V., Faluvegi, G., Folberth, G. A., Horowitz, L. W., Josse, B., MacKenzie, I. A., Nagashima, T., Plummer, D. A., Righi, M., Rumbold, S. T., Stevenson, D. S., Strode, S. A., Sudo, K., Szopa, S., and Zeng, G.: Analysis of present day and future OH and methane lifetime in the ACCMIP simulations, Atmos. Chem. Phys., 13, 2563–2587, https://doi.org/10.5194/acp-13-2563-2013, 2013.

Winterstein, F., Tanalski, F., Jöckel, P., Dameris, M., and Ponater, M.: Implication of strongly increased atmospheric methane concentrations for chemistry–climate connections, Atmos. Chem. Phys., 19, 7151–7163, https://doi.org/10.5194/acp-19-7151-2019, https://www.atmos-chem-phys.net/19/7151/2019/, 2019.

Wunch, D., Toon, G. C., Blavier, J.-F. L., Washenfelder, R. A., Notholt, J., Connor, B. J., Griffith, D. W. T., Sherlock, V., and Wennberg, P. O.: The Total Carbon Column Observing Network, Philosophical Transactions of the Royal Society of London A: Mathematical, Physical and Engineering Sciences, 369, 2087–2112, https://doi.org/10.1098/rsta.2010.0240, http://rsta.royalsocietypublishing.org/content/369/1943/2087, 2011.